

Predicting marine and aeolian contributions to the Sand Engine's evolution using coupled modelling

van Westen, Bart; Luijendijk, Arjen P.; de Vries, Sierd; Cohn, Nicholas; Leijnse, Tim W.B.; de Schipper, Matthieu A.

DOI

[10.1016/j.coastaleng.2023.104444](https://doi.org/10.1016/j.coastaleng.2023.104444)

Publication date

2024

Document Version

Final published version

Published in

Coastal Engineering

Citation (APA)

van Westen, B., Luijendijk, A. P., de Vries, S., Cohn, N., Leijnse, T. W. B., & de Schipper, M. A. (2024). Predicting marine and aeolian contributions to the Sand Engine's evolution using coupled modelling. *Coastal Engineering*, 188, Article 104444. <https://doi.org/10.1016/j.coastaleng.2023.104444>

Important note

To cite this publication, please use the final published version (if applicable). Please check the document version above.

Copyright

Other than for strictly personal use, it is not permitted to download, forward or distribute the text or part of it, without the consent of the author(s) and/or copyright holder(s), unless the work is under an open content license such as Creative Commons.

Takedown policy

Please contact us and provide details if you believe this document breaches copyrights. We will remove access to the work immediately and investigate your claim.



Predicting marine and aeolian contributions to the Sand Engine's evolution using coupled modelling

Bart van Westen^{a,b,*}, Arjen P. Luijendijk^{a,b}, Sierd de Vries^b, Nicholas Cohn^c, Tim W.B. Leijnse^{a,d}, Matthieu A. de Schipper^b

^a Deltares, Delft, The Netherlands

^b Faculty of Civil Engineering and Geosciences, Department of Hydraulic Engineering, Delft University of Technology, Delft, The Netherlands

^c U.S. Army Engineer Research and Development Center, Coastal and Hydraulics Laboratory - Field Research Facility, Duck, NC, USA

^d Institute for Environmental Studies (IVM), Vrije Universiteit Amsterdam, Amsterdam, The Netherlands

ARTICLE INFO

Dataset link: <https://doi.org/10.4121/collectio.n.zandmotor>

Keywords:

Morphodynamics
Mega nourishment
Numerical modelling
AeoLiS
Delft3D Flexible Mesh
Coupled modelling

ABSTRACT

Quantitative predictions of marine and aeolian sediment transport in the nearshore–beach–dune system are important for designing Nature-Based Solutions (NBS) in coastal environments. To quantify the impact of the marine-aeolian interactions on shaping NBS, we present a framework coupling three existing process-based models: Delft3D Flexible Mesh, SWAN and AeoLiS. This framework facilitates the continuous exchange of bed levels, water levels and wave properties between numerical models focussing on the aeolian and marine domain. The coupled model is used to simulate the morphodynamic evolution of the Sand Engine mega-nourishment. Results display good agreement with the observed aeolian and marine volumetric developments, showing similar marine-driven erosion from the main peninsula and aeolian-driven infilling of the dune lake. To estimate the magnitude of the interactions between aeolian and marine processes, a comparison between the simulated morphological development by the coupled and stand-alone models was made. This comparison shows that aeolian sediment transport to the foredune, i.e. 214,000 m³ over 5 years, extracts sediment from the marine domain. As a result, the alongshore redistribution of sediment from the main peninsula by marine-driven processes decreased by 70,000 m³, representing 1.7% of the total marine-driven dispersion. From the aeolian perspective, marine-driven deposition and erosion reshape the cross-shore profile, controlling the supply-limited aeolian sediment transport and the magnitude of sediment deposition in the foredunes. In the region with persistent accretion along the Sand Engine's southern flank, a higher than average foredune deposition was predicted due to morphological development of the region where sediment is picked up by aeolian transport. Including these marine processes in the coupled model resulted in an increase of 1.3% in foredune growth in year 1 and up to 6.7% in year 5 along this accretive section. At the northern flank, where the developing lagoon and tidal channel provided increased shelter to the supratidal beach, predicted foredune deposition reduced up to –11.5% over the evaluation period. Our findings show that both aeolian and marine transports impact reshaping the nourished sand, where developments in one domain affect the other. The study findings echo that the interplay between aeolian- and marine-driven morphodynamics could play a relevant role when predicting sandy NBS.

1. Introduction

In recent years, Nature-Based Solutions (NBS) have become increasingly popular soft engineering features which provide ecosystem services and add coastal resilience to coastal areas (Sutton-Grier et al., 2015; de Vriend et al., 2015; Stive et al., 2013; van der Meulen et al., 2014; Barciela Rial, 2019). NBS, which may include constructed beach

and dune features, are designed to be dynamic and their subsequent morphologic evolution is governed by the interplay of hydrodynamic, morphodynamic and ecological processes on timescales of hours to decades (van der Meulen et al., 2023). Therefore, to successfully design and predict the long-term benefits of coastal NBS, it is necessary to have a (a) comprehensive understanding of and (b) quantitative predictive

* Corresponding author at: Deltares, Delft, The Netherlands.

Linkedin: [bartvanwesten](#) (B. van Westen).

E-mail addresses: Bart.vanWesten@deltares.nl (B. van Westen), Arjen.Luijendijk@deltares.nl (A.P. Luijendijk), Sierd.deVries@tudelft.nl (S. de Vries), Nicholas.t.Cohn@usace.army.mil (N. Cohn), Tim.Leijnse@deltares.nl (T.W.B. Leijnse), M.A.deSchipper@tudelft.nl (M.A. de Schipper).

<https://doi.org/10.1016/j.coastaleng.2023.104444>

Received 25 August 2023; Received in revised form 22 November 2023; Accepted 16 December 2023

Available online 27 December 2023

0378-3839/© 2024 The Authors. Published by Elsevier B.V. This is an open access article under the CC BY license (<http://creativecommons.org/licenses/by/4.0/>).

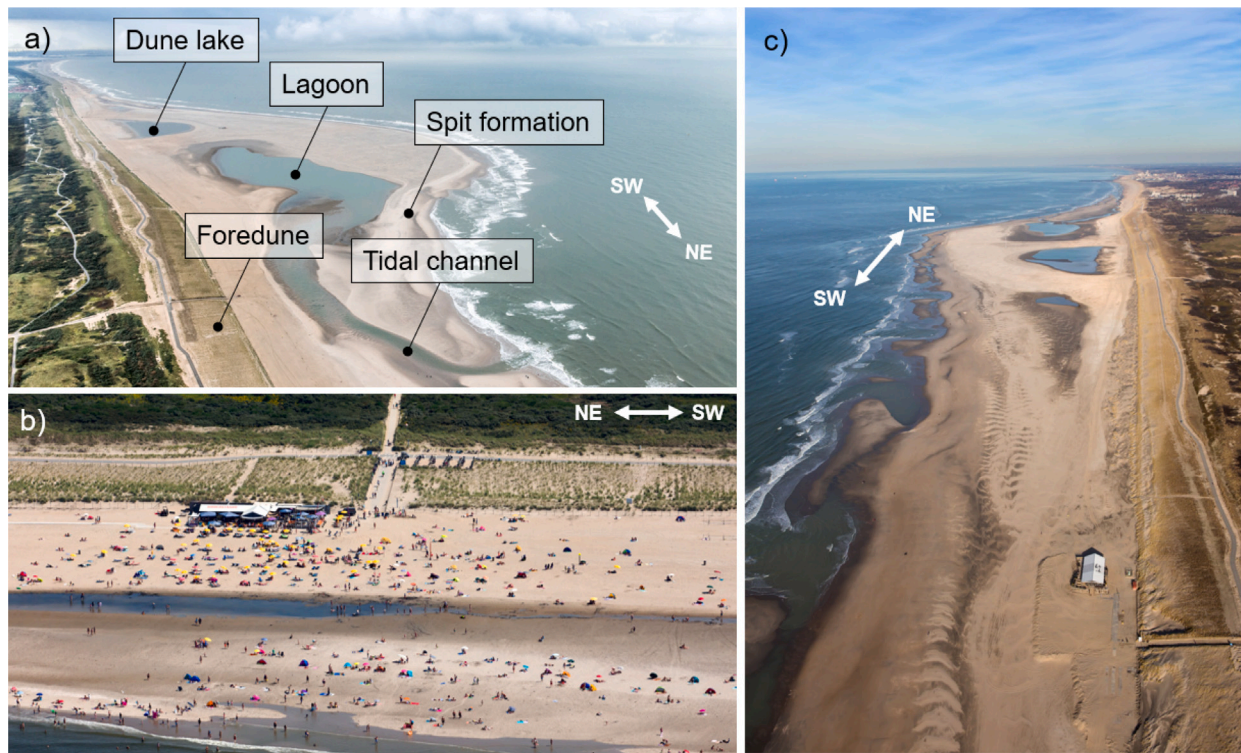


Fig. 1. Photos of the Sand Engine mega nourishment. (a) The Sand Engine one year post-construction, with the key geomorphological features. (b) Beachgoers at the Sand Engine's northern flank with the foredune in the back. (c) The southern flank of the Sand Engine 5 years after construction. The white arrows illustrate the Sand Engine's orientation, pointing towards the Northeast (NE) and Southwest (SW).

Source: Photo credits: Rijkswaterstaat/Joop van Houdt and Jurriaan Brobbel.

tools that can resolve the drivers of sediment transport gradients across the foreshore, surfzone, beach and dunes (Cohn et al., 2019; Luijendijk and van Oudenhoven, 2019; Bridges et al., 2021).

Shoreface and beach nourishments are widely used in erosive coastal systems to buffer storm impacts and add recreational and ecological value (de Schipper et al., 2021). While the placement of sand has been globally adopted to enhance coastal resilience, recently, mega-nourishments have been trialled to add immediate local and long-term far-field benefits through leveraging the longshore redistribution of placed sediments. An example of this type of NBS is the Sand Engine, a 21.5 Mm³ hook-shaped mega-nourishment, constructed in 2011 along the Delfland coast in the Netherlands (Stive et al., 2013, Fig. 1). Since its construction, many studies have monitored, analysed, and modelled the Sand Engine's evolution (de Schipper et al., 2016; Luijendijk et al., 2017; Tonnon et al., 2018; Roest et al., 2021). The Sand Engine was constructed with various goals, from nourishing the adjacent coast, to promoting dune growth, and enhancing the region's natural and recreational values. However, successfully predicting volumetric changes in the different parts of the NBS, and thus effectively accomplishing these diverse objectives, has proven challenging. During the design phase, it was estimated that the foredune growth in the Sand Engine's direct vicinity would approximately double the dune growth compared to the original situation (Mulder and Tonnon, 2011). This estimation was based on an empirically developed relationship between dunefoot migration and beach width (de Vriend et al., 1989). In practice, foredune deposition at the Sand Engine was measurably lower than along the adjacent coast in the years following the mega nourishment construction (Hoonhout and de Vries, 2017; Huisman et al., 2021).

Hoonhout and de Vries (2017) linked the observed reduction in foredune growth along the Sand Engine to supply limitations. While the theoretical rate of saturated, wind-driven sediment transport is a function of local grain size and wind speed (Bagnold, 1937; Sørensen, 2004; Sherman and Li, 2012), numerous factors may limit supply in

coastal environments and reduce local aeolian sediment transport rates below the theoretical maximum rate of saturation (de Vries et al., 2014b). This finding is consistent with multiple studies from other field sites that have found that the observed volumetric growth of coastal dunes is typically lower than that predicted from the wind-driven potential transport capacity (de Vries et al., 2014a; Costas et al., 2020).

Supply limiting conditions in coastal environments can especially be attributed to surface moisture (Hallin et al., 2023) and sediment sorting (van IJendoorn et al., 2023b). The wetting of the surface in the intertidal zone due to wave runup and groundwater effects results in an increased wind velocity threshold for initiating aeolian transport (Bauer et al., 2009; Ruessink et al., 2022; Hallin et al., 2023). Despite this constraint on aeolian transport near the land–water interface, the intertidal zone is often considered the primary source of sediment contributing to dune growth (Houser, 2009; Hoonhout and de Vries, 2017). Both within the intertidal zone and higher up on the dry beach, aeolian sediment transport can result in armouring of the bed as fine grain sediment is winnowed from the bed surface, preferentially leaving behind a layer of coarse material at the surface (i.e. lag deposits) that similarly contributes to supply limitations (Carter, 1976; Hoonhout and de Vries, 2017). At elevations lower than the total water level elevation, however, wave-induced forces can mix different sediment fractions, removing potential armouring and thus enabling more sediment supply (van IJendoorn et al., 2023a,b).

Since the intertidal zone is a primary zone of sediment pickup for wind-driven sediment transport, marine-driven sediment supply towards the intertidal zone can positively enhance aeolian transport rates (Aagaard et al., 2004). Cohn et al. (2017) showed that the landward migration and welding of breaker bars can contribute to rapid beach growth, which some studies have related to enhanced dune growth (e.g., Houser, 2009) perhaps due to the introduction of finer grained sediments and widening of the beach which reduced fetch limitations. These factors may similarly explain why aeolian transport and

net dune growth rates are often higher immediately following beach nourishments (van Rijn, 1997; van der Wal, 2004; Arens et al., 2013b). High energy events (i.e. storms) can induce beach and dune erosion, potentially adversely impacting the intertidal sediment budget (Quartel et al., 2008; Costas et al., 2020; González-Villanueva et al., 2023), potentially stimulating aeolian transport as a consequence of increased intertidal width and subsequent sediment availability. Aeolian pickup from the intertidal zone also modifies the intertidal sediment budget. To date, it is unclear to what extent removing this sediment by aeolian transport affects marine-driven transport through changes in grain size and morphodynamic feedback.

The multitude of interactive processes and scales hampers quantifying the impact of aeolian and marine interactions on long-term morphological development (Aagaard et al., 2004; Bauer et al., 2009; Moulton et al., 2021). As a result, the current understanding of the nearshore–beach–dune system primarily relies on observations, and conceptual and rule-based models, describing relations between the marine and aeolian domains (Short and Hesp, 1982; Sherman and Bauer, 1993; Bauer and Davidson-Arnott, 2003; Aagaard et al., 2004; Houser, 2009; Silva et al., 2019; Hallin et al., 2019a; Costas et al., 2020; Pellón et al., 2020; González-Villanueva et al., 2023). Despite the conceptual understanding of the impact that interactions between marine and aeolian processes have on coastal evolution, quantitative tools are still lacking.

To quantify marine-driven influences on aeolian developments, a fetch-based approach can be used (Bauer and Davidson-Arnott, 2003; Delgado-Fernandez, 2010; Ruessink et al., 2022). This approach is based on the concept that some critical fetch distance in downwind direction is needed to reach the wind-driven transport capacity. Sediment transport is limited in relation to the transport capacity by the limited distance (smaller than the critical fetch distance) in the direction of the wind relative to the waterline. This approach (over)simplifies the dynamic, time-varying conditions such as tidal excursion and storm events and does not take the impact of the system's evolving morphology on supply-limiters into account (Houser, 2009). Semi-empirical models describing beach-dune dynamics, like the CS-model developed by Larson et al. (2016), use a combination of physics and empirical observations to simulate the cross-shore exchange of sand and the consequent profile development. Building upon this, Zhang and Larson (2022) incorporated dune erosion into the model using the wave impact theory described by Larson et al. (2004). This model has proven fast and effective in predicting the evolution of beach-dune systems on yearly to decadal timescales (Palalane et al., 2016; Hallin et al., 2019b). However, its semi-empirical nature introduces a degree of site-specificity to some coefficients, necessitating data for calibration to ensure confidence in its application to specific locations. This aspect compromises the predictive ability in environments where data is scarce or when designing complex and novel NBS.

Process-based models have proven their use in quantitatively predicting the effects of natural events and human interventions on coastal evolution, e.g. at the Sand Engine (Luijendijk et al., 2017; Hoonhout and de Vries, 2019). Yet, most of these coastal process-based models mainly focus on distinct sub-domains, analysing either the marine (Warren and Bach, 1992; Booij et al., 1999; Hervouet and Bates, 2000; Lesser et al., 2004; Roelvink et al., 2009) or the aeolian (Durán et al., 2010; Keijsers et al., 2016; Hoonhout and de Vries, 2017) domains separately. Consequently, these models often neglect the interactions between aeolian and marine subdomains.

Integrating morphodynamic evolution across subdomains requires a tool that allows for the simultaneous prediction of multiple subdomains and a continuous exchange of morphological and hydrodynamic information between these domains. Several studies have made progress towards such integration. Roelvink and Costas (2019) included integrated dune development mechanics into the hydrodynamic XBeach model (Roelvink et al., 2009). The WindSurf framework (Cohn et al.,

2019) employed a coupling between XBeach and the aeolian transport model AeoliS (Hoonhout and de Vries, 2016). These frameworks proved valuable in advancing the understanding of interactions within the nearshore–dune system and showed the added value in adding them (Hovenga et al., 2023; van Westen et al., 2023). However, a common limitation of these coupling frameworks is the prerequisite that the submodels have to operate on the same, one-dimensional cross-shore grid. Depending on spatiotemporal scale, longshore variations could significantly contribute to the overall development coastal environments. Also, different parts of the coastal domain could require descriptions of different levels of detail. Therefore, to simulate real-world coastal environments, a numerical coupling tool is required that supports two-dimensional subdomains, regardless of their respective grid resolution or type. Luijendijk et al. (2019) solved this by proposing a coupling between Delft3D (Lesser et al., 2004) and AeoliS (Hoonhout and de Vries, 2016) models, both covering two-dimensional domains. Luijendijk et al. (2019) demonstrated the ability to include the interactions between the marine and aeolian morphodynamics by coupling these numerical models. However, a detailed analysis of the impact of these interactions on the system's integrated morphodynamics was lacking. Besides, limited spatial resolution restricted the model from including detailed aeolian landforms, e.g. foredunes, in this initial study.

The current study extends the current numerical frameworks and focuses on quantifying volumetric changes in the aeolian and marine parts of the Sand Engine to explore interactions between marine- and aeolian-driven portions of the study site. The impact of these interactions on the system's integrated morphodynamics is studied using a 2D coupled model encompassing both aeolian and marine domains. We define two Research Objectives:

1. The development of a coupling framework that enables simultaneous modelling of the aeolian and marine domains in 2D, thereby introducing the interactions between marine and aeolian morphodynamics;
2. Estimating the magnitude of the interactions between marine and aeolian morphodynamics and their impacts on the Sand Engine's evolution.

The development of this Delft3D-SWAN-AeoliS coupling framework facilitates simultaneous computation of multiple subdomains, including potential interactions that cross the land–sea boundary. Individual model components can successfully provide predictions of net landscape change of the subaerial (AeoliS) and subaqueous (Delft3D-SWAN) portions of the coastal zone, but independent models inherently ignore part of the sediment budget. For example, large amounts of sediment that are being deposited in the Sand Motor dune system would not be included in a budget analysis obtained from any stand-alone subaqueous model application or, vice versa, the subaqueous morphological development would lack in a model framework that only accounts for subaerial processes.

Due to interactions between the subdomains, we expect small deviations in morphological development to occur if the coupled model outcomes are compared to the sum of stand-alone outcomes. Since the individual model components have been specifically calibrated for standalone operation, we do not anticipate significant improvement of model skill in the central part of the domain the submodels were designed for. However, it might be expected that there are notable differences in the zones where both marine and aeolian processes operate, such as within the intertidal zone. This work aims to demonstrate new capabilities enabled by connecting multiple coastal domains within a single model framework that, through expanding both quantitative and qualitative understanding of system behaviour (Barbour and Krahn, 2004), allows for improved understanding of cross-domain interactions and integrated nearshore–beach–dune systems.

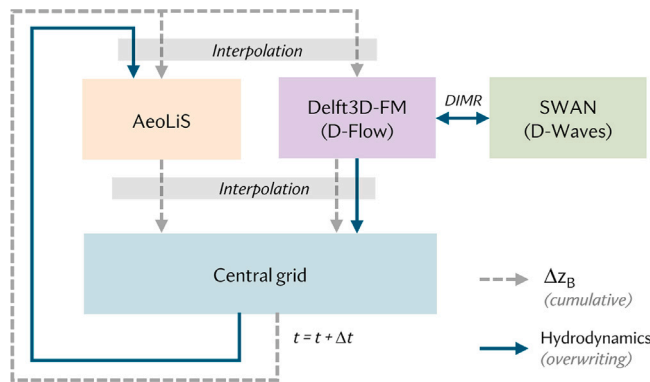


Fig. 2. Schematic representation of the parameter exchange settings between Aeolis (Hoonhout and de Vries, 2016) and Delft3D-FM model components (Lesser et al., 2004; Kernkamp et al., 2011). The arrows indicate the exchange of Δz_B (adding bed level change to existing bed elevation) and hydrodynamics (water levels, wave heights and wave period). The information is exchanged for every timestep Δt ($=1200$ s) in morphological time.

The coupling approach, the Sand Engine model set-up, model performance, and verification of the model results are described in Section 2. By analysing simulation results, we aim to predict the magnitude of the impact of marine and aeolian interactions on the Sand Engine's morphodynamic evolution (Section 3). To what extent our established Research Objectives are fulfilled is elaborated upon in the Discussion (Section 4), followed by the Conclusion (Section 5).

2. Coupled modelling of 5-year Sand Engine morphodynamics

2.1. Case study: the Sand Engine

The Sand Engine is a 21.5 Mm³ hook-shaped mega-nourishment constructed in 2011 along the Delfland coast (Stive et al., 2013), shown in Fig. 1. The average yearly northward alongshore sediment transport along the Delfland coast is estimated to be 0.38 Mm³, resulting from gross transports of 0.76 Mm³ northward and 0.38 Mm³ southward (van Rijn, 1995; de Schipper et al., 2016).

The Delfland has historically been retreating approximately 1 km inland from 1600 to 1990, as it faced structural erosion (de Schipper et al., 2016). After the Dynamic Preservation Act was implemented in 1990, mandating the maintenance of the 1990 coastline position (van Koningsveld and Mulder, 2004), nourishment construction started to increase. Before the Sand Engine's construction, nourishment volumes in this area rose to approximately 1.7 Mm³/year. The advantages thought of during its design, involving a high concentration of sediment nourishment at a single longshore location, are the reduced frequency of nourishments needed, the longshore spreading causing neighbouring shorelines to advance more naturally, the large initial land reclamation providing increased space for recreation activities and ecological development and the ecological stress remaining confined to a relatively small area, limiting its overall environmental impact (Stive et al., 2013).

For further information on the background, coastal setting, and governing conditions of the Sand Engine see Stive et al. (2013), de Schipper et al. (2016), Hoonhout and de Vries (2017) and Huisman et al. (2021).

2.2. Coupling approach

The framework presented in this study enables the coupling of three existing process-based models. This is achieved through the simultaneous execution of these models, hereafter model components, and the exchange of information between them. To achieve this, the Basic

Model Interface (BMI) protocol is utilized (Hutton et al., 2020), as it serves as an efficient way of coupling numerical models through the provision of dedicated functions.

Our work builds upon earlier studies that developed coupling tools for coastal applications. The initial BMI-enabled coupling framework is WindSurf as coded by Hoonhout (2016). WindSurf supports the coupling between one-dimensional Aeolis (Hoonhout and de Vries, 2016) and XBeach (Roelvink et al., 2009) models, with an application of these couplings presented in Cohn et al. (2019). Additionally, Luijendijk et al. (2019) utilized a similar BMI protocol to facilitate the exchange of parameters between two-dimensional model components. In this study, we have combined the generic structure of the BMI-version of the Windsurf framework (Hoonhout, 2016), with some of the model schematization and exchange methods from Luijendijk et al. (2019) to enable comprehensive 2D model coupling capabilities. A central grid is utilized as a communication layer between models, ensuring the model components are not required to have the same central model grid coordinates or resolution (Fig. 2). This method eliminates the need for setting up numerous individual exchanges between the multiple model components. Additionally, having one shared morphological state minimizes the discrepancy across model components. For our case study, the central grid is based upon the Delft3D-FM grid (Section 2.3.1, Fig. 3b).

To increase the flexibility and application range, the coupling framework is made compatible with different grid types (e.g., rectangular, curvilinear, unstructured). To enable the exchange of information between these grids, we implemented a re-gridding functionality, which is based on a simple linear interpolation method. The influence of the coupling and interpolation approach on mass-conservation will be reflected upon in Section 2.5.2.

2.3. Model components

The coupled model consists of three model components. Throughout the setup of our coupled model, we aimed to maintain the setups of each component as closely as possible to earlier Sand Engine research (Luijendijk et al., 2017; Hoonhout and de Vries, 2019) to minimize the effort required for setting up and calibrating the model components. Our main focus is on quantifying the added value of enabling interaction between models, instead of demonstrating the performance within the individual subdomains.

The primary hydrodynamic component, Delft3D Flexible Mesh (Kernkamp et al., 2011), hereafter Delft3D-FM, simulates sediment transport and morphological change in the marine domain (Fig. 3b) under the influence of tidal, wind, and wave-driven water levels and currents, following the methods of Lesser et al. (2004). The setup of Delft3D-FM is described in Section 2.3.1. The SWAN model (Fig. 3a) simulates the propagation and transformation of wind-generated waves (Booij et al., 1999) that is linked with Delft3D-FM through a wrapper called D-Waves, see Section 2.3.2. The morphological evolution in the aeolian domain (Fig. 3c), influenced by aeolian-driven, supply-limited transport, is simulated by the Aeolis model (Hoonhout and de Vries, 2016), see Section 2.3.3.

2.3.1. Delft3D-FM configuration

The configuration of the Delft3D-FM model component builds upon the Sand Engine simulations by Luijendijk et al. (2017). The computational domain covers an alongshore stretch of coast of nearly 20 km from Hoek van Holland to just north of Scheveningen (Fig. 3b). It extends approximately 15 km offshore. The cross-shore grid resolution is 1000 m at the offshore boundary and 35 m at the surfzone (Fig. 3b). Considering the width of the surfzone varying between approx. 150 m at the tip of the peninsula to 300 m along the more natural coast, the chosen cross-shore resolution results in at least 5 grid cells in the surfzone. To more accurately resolve detailed surf zone processes a finer resolution in the surfzone could be beneficial, but here we

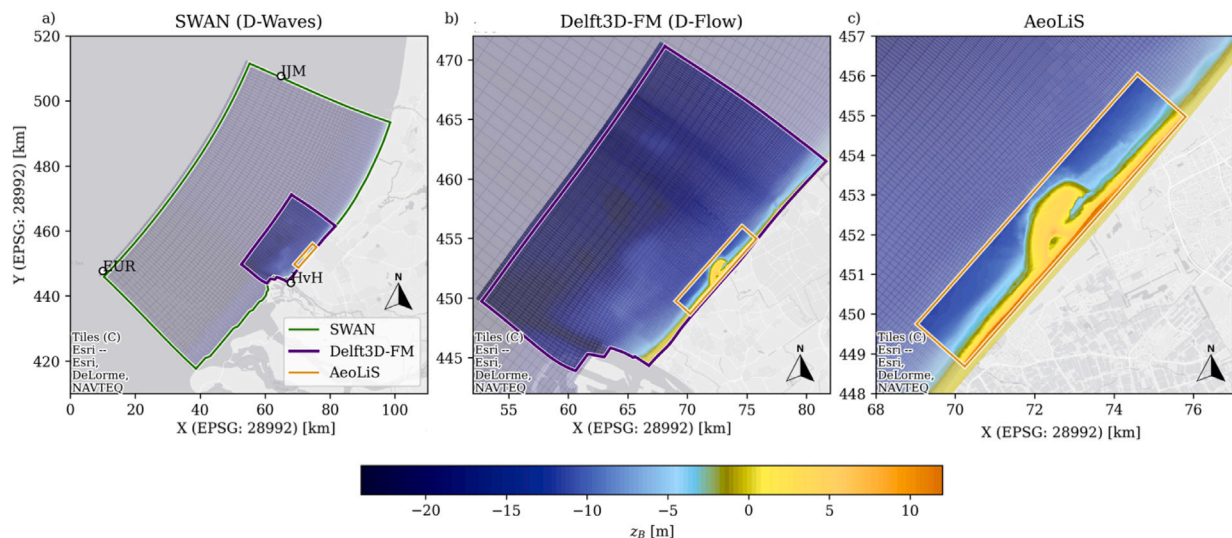


Fig. 3. Computational domains of SWAN (a, green), Delft3D-FM and refined SWAN (b, purple), and AeoliS (c, orange). HvH, EUR and IJM indicate the wind and offshore wave stations used for the wave boundary conditions. Colours indicate bed level with respect to NAP (Dutch datum at approximately mean sea level).

compromise between sufficiently detailed resolution to resolve dominant behaviour at the study site and non-exorbitant computational times. Among the processes that this resolution was optimized for was the ability to successfully capture longshore transport rates and the capacity of the model to reproduce the Sand Engine's historical dispersion. As shown in Section 2.6.1, the model effectively reproduces these longshore processes, hence justifying the chosen resolution. At the lateral boundaries, zero-gradient alongshore water level, or Neumann, conditions are enforced (Roelvink and Walstra, 2004).

The model has been upgraded from Delft3D version v4 (Lesser et al., 2004) to Delft3D Flexible Mesh solver (Kernkamp et al., 2011), allowing for more efficient grid refinement opportunities. This upgrade required a re-calibration of the sediment transport-related factors for suspended and bedload transport (sus and bed). To match the volume change within the main Sand Engine peninsula as modelled by Luijendijk et al. (2017), the values for sus and bed were set to 1.4 [-]. Additionally, the sediment transport factors for wave-driven transport ($susw$ and $bedw$) were set to 0.5 [-].

2.3.2. SWAN configuration

Like the Delft3D-FM configuration, the SWAN setup is based on Luijendijk et al. (2017). Two domains are used in a nesting approach. The larger wave domain extends ~10 km in both longshore directions (north and south) and ~15 km in offshore direction to adequately describe wave transformation. A finer grid that matches the Delft3D-FM grid is nested inside the larger grid (Fig. 3a, b), with an increased cross-shore resolution of roughly 35 m around the shoreline.

2.3.3. AeoliS configuration

The AeoliS setup primarily relies on the previous work by Hoonhout and de Vries (2019). The area of interest has been extended to cover a more extensive alongshore coastal stretch. Moreover, a finer grid, increasing the resolution from 50×50 m to 12.5×12.5 m (equidistant), is applied to acquire sufficient resolution for the simulation of foredune development. The offshore boundary of the AeoliS domain is defined by the edge of the aeolian zone, as indicated by the orange box in Fig. 3.

The influence of vegetation cover is included by locally reducing the shear stress following the methods of Durán and Moore (2013). In the absence of comprehensive spatial measurements of vegetation cover, vegetation presence and growth are currently implemented following simple rules based on general field observations. The vegetation coverage is determined based on the evolving bed level elevation [m] and slope [°]. No vegetation is present below 4m+NAP, while all cells

above 6m+NAP are fully covered. Between 4 and 6m+NAP, only cells with a bed slope of at least 24° are covered with vegetation. Including avalanching ensures that the bed slope does not exceed the imposed angle of repose (33°). These chosen values are iteratively determined to reproduce key aspects of the cross-shore profile evolution. This implementation resulted in a gradual and realistic seaward migration of the dunefoot, while maintaining a realistic foredune slope.

Due to the absence of run-up processes within the hydrodynamic model components, AeoliS uses the regridded wave characteristics to calculate wave run-up, based on the empirical formula by Stockdon et al. (2006). While the Stockdon et al. (2006) formula fundamentally relies on offshore wave heights, in the present setup, local wave conditions are employed. Since the local wave height is lower than the offshore conditions due to wave breaking, this approach is expected to lead to an underestimation of wave run-up and subsequently in a smaller area of inundation.

2.4. Setup of the 5-year model hindcast

The coupled model is tailored to simulate the morphological development of the Sand Engine for the first 5 years after construction, from August 1st, 2011, to August 1st, 2016. All three model components use the same initial topographic and bathymetric data. The description of obtaining and processing this bed elevation data for input to the models is added to Appendix A.

2.4.1. Parameter exchange

The coupling interval of the parameter exchange between the model components is 1200 s in morphological time. Bed levels are continuously exchanged between Delft3D-FM and AeoliS to include the morphodynamic interactions between the aeolian and marine domains. To reduce the impact of continuously overwriting bed levels on mass conservation and preservation of details involving grids of different dimensions and resolutions, the bed level change is computed using a cumulative approach. This means that rather than repeatedly replacing existing bed levels with new values calculated by the Delft3D and AeoliS model components after ($z_{B,central}[t] = z_{B,model}[t]$), we update the bed level of the central grid incrementally, adding only the calculated change in bed level, Δz_B [m] ($z_{B,central}[t] = z_{B,central}[t-1] + \Delta z_{B,model}[t]$). This process is facilitated by tracking the changes in bed level calculated by different model components during each step.

To incorporate the marine-driven sediment supply-limiters on aeolian transport dynamics, including the aforementioned hydrodynamic

reworking of grain size distributions in the swash zone and soil moisture content of the bed surface from wave runup, the water levels z_s [m+NAP], wave height H_s [m], and wave period T_p [m] are exchanged from Delft3D-FM to AeoliS through the central grid. The exchange of wave-related information between Delft3D-FM and SWAN occurs through the DIMR-coupler (Deltares, 1982, Deltares Integrated Model Runner) with a coupling interval 3600 s in morphological time.

During simulations, we stored the marine- and aeolian-driven bed level change separately, allowing us to determine their relative contributions to the overall development. To exclude the aeolian- or marine-driven morphodynamics from the simulation results entirely, two additional simulations were conducted by disabling the bed level updates from (1) the AeoliS model (see Fig. 3d–e) and (2) the Delft3D-FM model (see Fig. 3f–e). Despite not being fully uncoupled, these simulations are referred to as AeoliS-only or Delft3D-FM-only, respectively. By keeping the model components integrated within the coupling framework, we maintain the exchange of water levels and wave properties between the domains while eliminating morphodynamic interactions. This method ensures that deviations arising from information exchange and re-gridding do not influence the outcomes of later comparative analysis.

2.4.2. Forcing conditions

The boundary conditions for the model set-up are generated following the methodology of Luijendijk et al. (2017). Alongshore variable astronomical tidal components are imposed on the offshore boundary of the hydrodynamic model and observed surge levels at Hoek van Holland are added to these tidal levels (Fig. 3a).

Wind speed and direction data are obtained from 10-minute averaged observations at Hoek van Holland. Wave characteristics are sourced from two offshore platforms: Europlatform and IJmuiden Munitiestortplaats (Fig. 3a). Data gaps in the wave timeseries from both offshore platforms are filled using information from the other platform. The remaining data gaps in wave (2%) and wind (7%) timeseries are filled with zero values. This conservative approach may result in a slight underestimation of wave- and wind-driven transport.

2.4.3. Upscaling techniques

The boundary conditions generated in this study undergo a series of processing procedures to reduce computational expenses by implementing filtering and acceleration techniques (Luijendijk et al., 2019).

The boundary conditions are filtered based on wave and wind criteria. First, periods with offshore-directed waves ($40^\circ\text{N} < H_{dir} < 200^\circ\text{N}$) and winds ($60^\circ\text{N} < u_{dir} < 180^\circ\text{N}$) are removed. Next, conditions are filtered based on wave height ($H_s < 1$ m: 49%) and wind speed ($u_{10} < 5.5$ m/s: 49%). The filtering criteria for wave height are based on Luijendijk et al. (2017). The wind speed is based on threshold velocity for the smallest sediment fraction (250 μm) to initiate aeolian transport, according to the applied transport formulation by Bagnold (1937). Conditions were only filtered out of the timeseries when all requirements were met simultaneously, resulting in a reduction of 39% of the total duration to be simulated, allowing for an increased computational speed of these comprehensive 2D simulations.

To further accelerate the simulation, a morphological acceleration factor of 3 is applied in Delft3D-FM simulation, hereafter referred to as *morfac* (Ranasinghe et al., 2011). AeoliS's smaller computational costs remove the need for applying acceleration techniques on the AeoliS model component within this setup. To align the morphological timeframes of both model components, which operate with different *morfac*s, the coupling interval is adjusted for each component.

2.5. Evaluation of coupling approach

With the coupled model being set up and run for the 5-year period, we evaluate some key performance aspects of the coupled model compared to the model components.

2.5.1. Preservation of detail

To retain relevant aeolian landform information, such as foredune profile characteristics, the level of detail required by AeoliS (12.5 m) surpasses that implemented in Delft3D-FM (finest grid resolution of 35 m). Therefore, it is important to ensure that during the transfer of information from the coarser Delft3D-FM grid to the finer AeoliS grid, no details regarding the shapes of aeolian landforms are averaged out. As the central grid shares a similar cross-shore resolution with the AeoliS grid, no information is lost when transferring the bed level data from the central to the AeoliS grid. Likewise, as we only add bed level changes from Delft3D-FM to the bed level stored in the central grid, we retain the detail of the bed topography from the previous timesteps.

2.5.2. Mass-conservation

The coupling framework's ability to conserve mass is assessed by computing the net volumetric change based on the bed level changes introduced by individual model components and comparing it to the combined volumetric change. Over the 5-year simulation period, the bed level changes induced by Delft3D-FM resulted in a total net loss of 542,970 m^3 and AeoliS induced a loss of 4,864 m^3 . The total volumetric loss resulting from the individual model components is thus 547,834 m^3 . These net volume changes result from sediment fluxes leaving the landward, offshore, or onshore boundaries of the computational domains. The total volumetric loss based on the coupled simulation result is 543,230 m^3 , which is 4,605 m^3 less than the sum of the individual model components. This surplus of sediment in the coupled simulation is likely to be the result of the linear interpolation method. Although the chosen method appears to be not fully mass-conservative, the volumetric deviation is small enough ($< 1\%$ of the net total losses) to assume that the impact on our main objective is negligible.

2.5.3. Computational costs

Continuous or frequent data exchange in the coupling framework could lead to significant computational costs due to the overhead associated with model input/output and re-initialization. To mitigate model slowdowns and enable efficient multi-year simulations, we employed pre-computed weight matrices that map the results from the model components to the central grid and vice versa. These weight matrices are generated based on the earlier described linear interpolation method. The total computation time for the 5-year hindcast can be separated into time for AeoliS (17.5%), Delft3D-FM (70.4%), and SWAN (11.1%). The remainder, only 1.0% of the total computational time, is attributed to the coupling framework itself.

2.6. Data-model comparisons

We evaluate the coupled model's ability to reproduce the observed aeolian and marine landform evolution. The model components have previously been calibrated on the Sand Engine study site, and their predictive proficiency for their respective subdomains has been demonstrated (Hoonhout and de Vries, 2019; Luijendijk et al., 2017). In this study, our focus is on the added value created by enabling interactions between these domains.

Comparing the model and measurement results, we find that the model accurately reproduces the observed erosion and deposition patterns in the nearshore domain (Fig. 4d vs. 4j; see Section 2.6.1 for quantitative comparison). The shoreline retreat along the Sand Engine's main body, adjacent accretion, and overall development into a Gaussian-shaped platform correspond well with the observations (Fig. 4c vs. 4i). At the Sand Engine's tip ($x=900$ m in Fig. 5), the shoreline ($z_B = 0$ m+NAP) retreated with 350 m after 5 years, which is slightly underestimated by the coupled model with 325 m. Just south of the Sand Engine ($x=-50$ m in Fig. 5), the shoreline has moved 120 m seaward, which is overestimated by the model with 180 m. The model's inability to simulate the cross-shore profile shape accurately

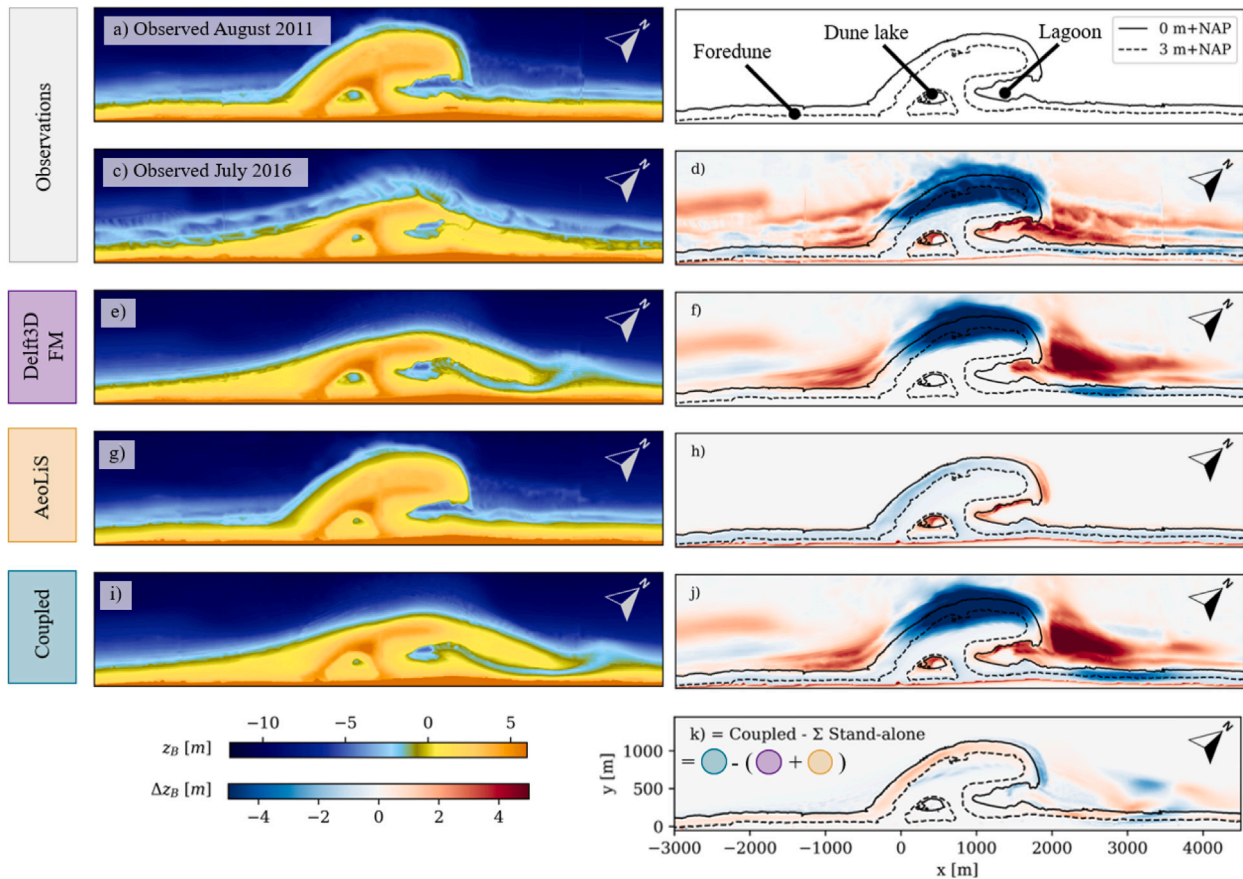


Fig. 4. Comparison between the modelled and observed morphological development. (a) The initial bed level just after construction and (b) contour lines after construction and key features. (c,d) The observed bed level and bed level change after 5 years. Modelled bed level and bed level change for Delft3D-FM-only (e,f), Aeolis-only (g,h) and coupled (i,j) simulations. Panel (k) shows the difference between the coupled simulation results and the sum of both stand-alone simulations.

is likely to affect these outcomes. The construction of the Sand Engine has resulted in the formation of sandbars at a depth of approximately $-m+NAP$ (Rutten et al., 2018; Huisman et al., 2021). The model does not include these features, as the cross-shore profile is smoothed out (Fig. 5c). We expect this to result from typical 2DH process-based (Delft3D) model shortcomings.

The largest discrepancies are found north of the Sand Engine. Although the existence of the northern spit-like feature and the closure of the lagoon, along with the formation of a tidal channel, are included in the model results, some precision is lacking (Fig. 4c vs. 4i). In the model results, the shoreline along the spit extends 305 m further seaward compared to observations ($x=2000$ m in Fig. 5). This discrepancy is likely to be linked to the overestimation of the width and depth of the simulated tidal channel. The lowest observed bed level elevation within the tidal channel remains above 0 m+NAP, while the modelled tidal channel reaches a bed level lower than -1.5 m+NAP. We expect that the lack of run-up and overwash-related processes, in combination with a coarse cross-shore resolution, causes these deviations.

Along the entire domain, the observed upper beach remains relatively stable. Along the accretive southern flank (transect B, Fig. 5), the observed average bed level elevation of the upper beach ($1 < z_B < 4$ m+NAP) is 2.2 m+NAP. Meanwhile, the model predicts erosion within the same area, resulting in an average bed level of 1.7 m+NAP.

Aeolian sediment deposition along the edges of the dune lake, lagoon, and foredune ridge, locally accumulates up to over 5 m vertically and is visually similar between the model and measurements (see Section 2.6.2 for quantitative comparison).

In summary, visually, the simulation results of the coupled model align well with observations in both the aeolian and marine domains.

This was already the case for the existing stand-alone simulations (Fig. 4d–e vs. 4f–g). However, the continuous exchange of information between the two subdomains has allowed the incorporation of the non-linear interactions between aeolian- and marine-driven morphodynamics. The sum of the two stand-alone simulations deviates from the coupled model results, as shown in Fig. 4k. The largest differences can be observed within the intertidal area and along the northern spit, where the interaction between the aeolian and marine domains naturally is most prominent. The consequences of enabling these aeolian-marine interactions will be elaborated upon in Section 3.

2.6.1. Marine domain

To assess the model's ability to simulate marine developments, we examined the total eroded volume from the original Sand Engine domain and the corresponding accretion to the adjacent domains (Fig. 6a).

The model forecasts a total erosion volume of 4.1 Mm³ from the main peninsula (blue in Fig. 6a) over 5 years, slightly overestimating the observed volume of 3.9 Mm³ by 4.6% (Fig. 6b). Notably, the erosion from the marine domain diminishes over time, with the initial year showing particularly pronounced erosion (Roest et al., 2021). This trend is largely attributable to a stormy year and high initial shoreline gradients.

On the other hand, the model underestimates the accretion to the south of the Sand Engine, shown in green in Fig. 6b (observed: 1.6 Mm³, modelled: 1.4 Mm³, -11.9%). Similar to the earlier visual comparison, the most significant deviations occur north of the Sand Engine, where the model overestimates the northward spit development, shown in pink in Fig. 6b (observed: 1.9 Mm³, modelled: 2.6 Mm³, $+38\%$).

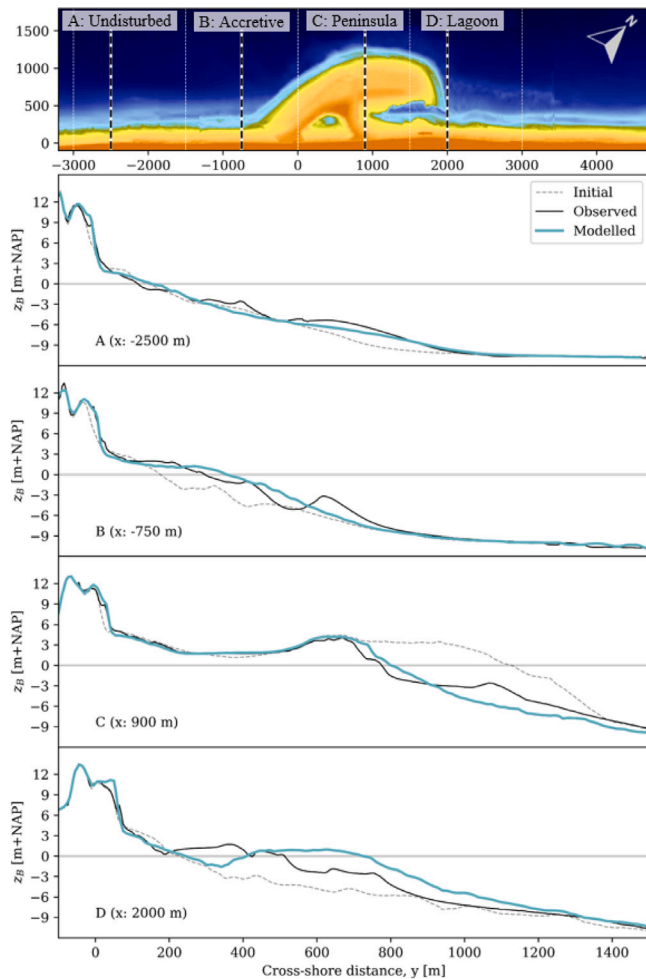


Fig. 5. Comparison between the modelled and measured cross-shore development for four transects within Sections A to D. The dotted, continuous black and continuous blue lines show the initial, observed and modelled bed levels, respectively.

2.6.2. Aeolian domain

To evaluate the model's ability to replicate aeolian sediment fluxes, we compared the modelled volume change within the dune lake domain to observations. The dune lake acts as a large catchment area for sediment transport driven exclusively by aeolian processes, regulated by both transport- and supply-limiting conditions.

We examined the volume changes within the dune lake region of influence, being the lake and the surrounding moist bed. We used the area enclosed by the 3 m+NAP isobath after construction as the region of influence (Fig. 6c, blue patch) as it matches the extend of the moist zone seen in satellite imagery.

The coupled model accurately reproduces the spatial pattern of deposition around the edge of the dune lake, with most deposition in the south-western part of the lake, corresponding with the direction of the most prevalent winds (Fig. 6d vs. 6e). The simulated volume change within the dune lake domain slightly underestimates the observed infilling (−15%, Fig. 6d). This discrepancy primarily arises during the first year. In subsequent years, the model better follows the observed trend.

3. Marine and aeolian process interactions

Building upon the demonstration of the coupled models' capability, we now use the model to analyse how the aeolian and marine domains influence each other. During the analysis, we divided the evaluation

domain into four distinct sections, A through D, each spanning 1500 meters and possessing unique characteristics, as depicted in Fig. 7. Section A is considered to be beyond the Sand Engine's influence zone. Section B is subject to progradation of the shoreline originating from the main peninsula. Section C includes the main peninsula itself and is marked by significant beach erosion. Lastly, Section D encompasses the area where the spit and tidal channel are developing.

3.1. Aeolian and marine contributions

Both aeolian and marine processes influence the morphodynamic evolution of the Sand Engine. However, the magnitude of these processes differs in longshore and cross-shore directions. The longshore and cross-shore average bed level changes Δz_B [m] as computed by the coupled model are separated and individually examined in Fig. 7. Aeolian-driven bed level changes are typically an order of magnitude smaller than those driven by marine processes. Averaged over the cross-shore profile ($-50 \text{ m} < y < 1450 \text{ m}$) the aeolian-driven bed level changes vary in the longshore direction from -0.22 to $+0.18 \text{ m}$ (Fig. 7, bottom panel). These are substantially smaller than those driven by marine processes ranging from -1.51 to $+0.98 \text{ m}$.

By averaging over the alongshore direction (Fig. 7, left panel) the data shows that, near the foredune, the averaged bed level change is comparable in magnitude to marine-driven variations (both of order 1 m).

For a deeper exploration of aeolian and marine interactions in the intertidal domain, we examined the accretive region just south of the Sand Engine, section B (Fig. 8). The marine-driven supply from the Sand Engine peninsula towards the intertidal zone characterizes this section (purple in Figs. 7 and 8c). This deposited sediment is pickup up by aeolian processes and transported to the foredune (the orange patch in Fig. 8c), illustrating the mutual exchange of sediment through the intertidal domain. The new dunes landward of the nourishment have been planted with marram grass (Fig. 1b,c). Sedimentation has been observed at the base of this artificial dune, where grasses are capable of trapping sediment and using sand burial for enhanced growth (Nolet et al., 2018). Although minor deviations exist between the model and measurement results (Fig. 8a, black vs. blue lines), the main accretive pattern is similar. However, zooming in on the supratidal area (Fig. 8b) reveals that the model predicts erosion from this higher elevated beach, which is not evident from the measurements. In total, the bed level elevation of the aeolian zone, being the primary source for aeolian transport along Section B ($20 \text{ m} < y < 220 \text{ m}$, Fig. 8b) m, is underpredicted with 0.36 m.

3.2. Aeolian impact on longshore dispersion

The results above indicate that, although the magnitudes might differ, marine and aeolian processes shape the Sand Engine. In the upcoming sections, we aim to estimate the impact of the interactions between marine- and aeolian-driven morphodynamics on the system's integrated morphological development.

First, we evaluate the impact of aeolian processes on the primarily marine-driven longshore dispersion. We use the volumetric erosion from the peninsula (similar to Section 2.6.1 and Fig. 6b) to quantify the impact of aeolian-driven processes on marine-driven sediment transport.

During our 5-year evaluation period, the aeolian flux into the foredune along the Peninsula-polygon is $214,038 \text{ m}^3$. We expect this sediment to originate primarily from the intertidal domain, reducing sediment availability for marine-driven alongshore dispersion. We consider the marine-driven dispersion from the coupled simulation and compute the difference with the Delft3D-FM-only simulation (Section 2.4.1) to estimate the aeolian contribution to marine-driven dispersion. In the Delft3D-FM-only simulation, a total of 4.17 Mm^3 left the domain as a result of marine-driven transport. In the coupled simulation, the

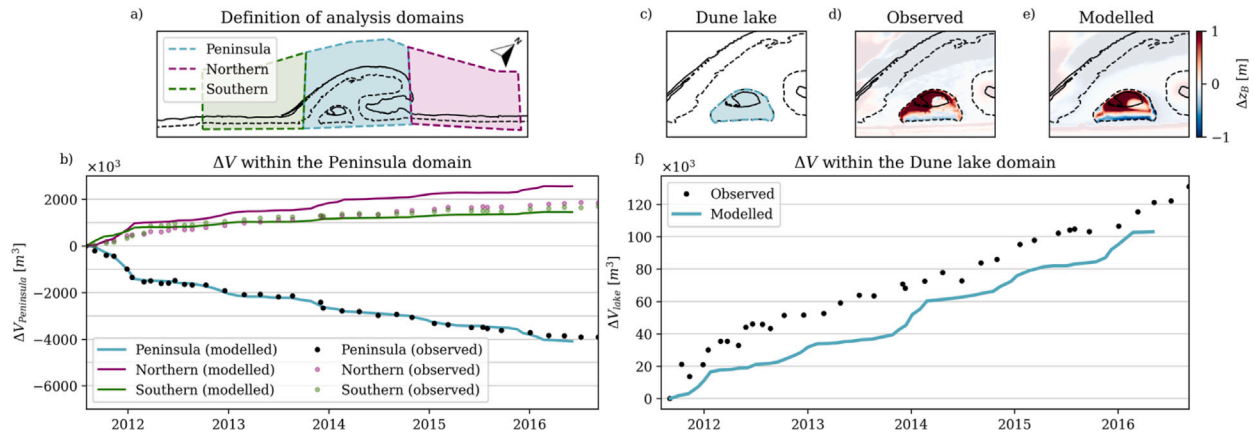


Fig. 6. Assessing the model’s ability to simulate the marine (a,b) and aeolian (c,d) domains. (a) The Peninsula (purple), northern (pink) and southern (green) analysis domains and (b) the volumetric change over time within these domains. (c) The dune lake domain is indicated in blue. The observed (d) and modelled (e) bed level changes around the dune lake for comparison. (f) The volumetric change over time within the dune lake domain.

marine-driven transport was 4.10 Mm³. This shows that the inclusion of aeolian transport reduces marine-driven dispersion by 69,661 m³, which is 1.7% of the total 4.17 Mm³. This reduction is relatively small compared to the total amount of sediment transported into the foredune (33% of 214,000 m³).

3.3. Marine impact on foredune deposition

Alongshore variations in foredune deposition are examined to map the influence of marine-driven processes on the aeolian domain. To further discern the influence of marine-induced morphodynamics on aeolian dune growth, we analysed the additional AeoliS-only simulation (Section 2.4.1). For this foredune deposition analysis, we excluded the region north of the Sand Engine ($x > 3000$ m, see Fig. 9b) since the beach entrances and restaurants heavily affect growth rates.

Within the central part of the modelled region (-3000 m $>$ $x > 3000$ m) the average dune growth amounts to 83.7 m³/m over a 5-year period, which is equivalent to 16.7 m³/m/year (Fig. 9b). The model slightly overestimates this net dune growth with a predicted alongshore average of 95.2 m³ over the 5-year period (19.0 m³/m/year). These measured and predicted growth rates fall within the typical range of Dutch dune growth, which varies from 0–0 m³/m/year (de Vries et al., 2012). We explore the alongshore variations in the observed and modelled foredune deposition using four distinct coastal sections broken up into 1,500 m alongshore increments (see sections A-D in Fig. 9b):

The “undisturbed” section (A: $-3000 < x < -500$ m) lies just south of the Sand Engine and is assumed to be located beyond the Sand Engine’s range of influence. The measured foredune growth here aligns with the domain average (88.9 m³/m/m), which the model closely reproduces at 92.6 m³/m/m.

The “accretive” section (B: $-1500 < x < 0$ m) is characterized by an accretive intertidal domain as a result of the longshore dispersion along the main peninsula. Observations show a noticeably higher dune growth rate in this region, averaging 110.2 m³/m (A→B: +24%) over 5 years. Though the model reflects this increase, it does so conservatively at 106.4 m³/m (A→B: +15%).

The peninsula-section (C: 0 m $<$ $x < 1500$ m), located behind the Sand Engine’s initial position, measured a foredune growth of 78.8 m³/m. This growth reduction of –11% with respect to the undisturbed section A contradicts initial predictions made during the Sand Engine’s design phase (Mulder and Tonnon, 2011), in which the used empirical relation anticipated a doubling of foredune growth. The observed depression in foredune deposition aligns with the longshore position of the dune lake (Fig. 9a-b). The centre of the foredune deposition depression ($x = 800$ m) is situated further north than the actual location of the dune lake ($x = 400$ m). We determined this centre by locating the point that stayed inundated the longest before accumulating the entire lake. The northward shift aligns with the prevailing wind direction, generally from south to southwest. The model overestimates dune growth slightly at 103.1 m³/m across the zone. However, the model successfully predicted the local depression landward of the dune

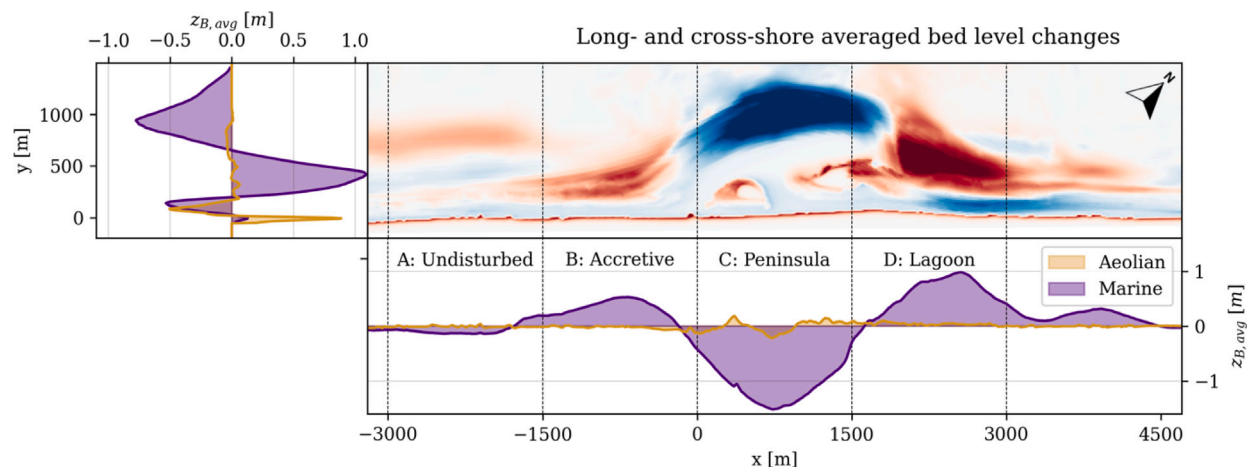


Fig. 7. The average bed level changes in long- and cross-shore direction due to marine (purple) and aeolian (green) processes.

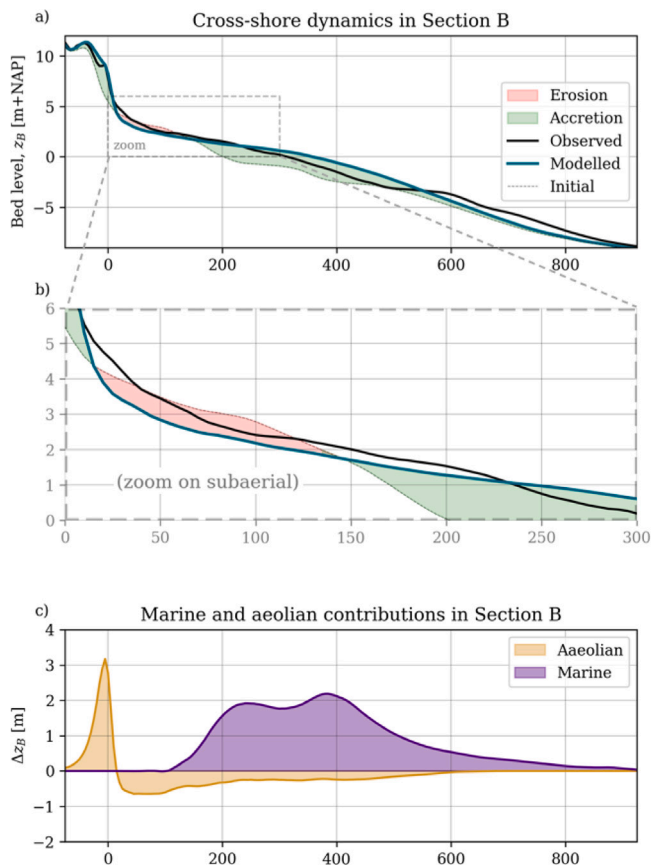


Fig. 8. The cross-shore varying dynamics within Section B (Accretive) over the 5-year period. (a) The observed and modelled cross-shore bed level changes (black and blue, resp.) are shown for the entire profile and (b) zoomed in on the aeolian part. (c) The purple and orange patches indicate the marine and aeolian contributions respectively.

lake and the more northward-located centre and accurately predicted dune growth at this depression centre (observed: $53.6 \text{ m}^3/\text{m}$, model: $56.9 \text{ m}^3/\text{m}$).

The lagoon-section (D: $1500 \text{ m} < x < 3000 \text{ m}$) shows a continuing decline in observed foredune growth towards the Sand Engine's lagoon and the adjacent tidal channel. Both measurements ($56.6 \text{ m}^3/\text{m}$) and model results ($78.9 \text{ m}^3/\text{m}$) record the lowest dune growth along the examined coastal stretch. The model successfully replicates the spatial patterns in dune growth, including the decline in volumetric gains towards the tidal channel, but generally underrepresents its magnitude (observed: $38.4 \text{ m}^3/\text{m}$, modelled: $52.2 \text{ m}^3/\text{m}$, +36%), and locates this decline it roughly 500 meters more to the north than field data capture. The model overpredicts dune growth in this zone by 39%.

The observed foredune deposition shows significant annual variability throughout the evaluation period (black bars in Fig. 9d-g). Especially the first year after construction shows a higher deposition rate. This is exemplified within the accretive region (section B), where dune growth reduces from 28.2 to $10.0 \text{ m}^3/\text{m}/\text{year}$ between years 1 and 2. Similarly, landward of the lagoon (section D), dune growth decays from $26.4 \text{ m}^3/\text{m}/\text{year}$ in year 1 to an average of $7.5 \text{ m}^3/\text{m}/\text{year}$ over the subsequent four years. The observed annual variability can be partly attributed to the temporal fluctuations in potential wind-driven transport, as indicated by the grey bars in Fig. 9d-g. Yet, the pronounced decrease in foredune growth from year 1 to 2, compared to the smaller decline in potential wind-driven capacity, underscores the influence of sediment availability on dune growth.

The model significantly overestimates dune growth in the first year (blue vs. black bars in Fig. 9d-g), which is particularly apparent in

Section C, the Sand Engine peninsula, where the initially modelled dune growth is $49.0 \text{ m}^3/\text{m}$ compared to the observed $25.9 \text{ m}^3/\text{m}$. Although these deviations are most prominent in the first year, significant deviations are also present in subsequent years. While the model captures the second and third years (2013 and 2014) reasonably well, it underestimates the annual growth in the last two years. In the accretive domain (section B), the observed dune growth in the final year is $23.7 \text{ m}^3/\text{m}$ compared to the model's prediction of $17.3 \text{ m}^3/\text{m}$.

Comparing the coupled simulation and AeoliS-only results enables us to estimate the impact of the marine-driven morphodynamic development on the longshore variations in foredune deposition (see orange line in Fig. 9c). Along Sections A and B, the coupled model predicts slightly higher foredune deposition than the AeoliS-only results (2.3% and 3.5%, respectively). The local increase in foredune deposition indicates a positive impact that marine-driven morphodynamics have on the sediment availability for aeolian transport. On the contrary, in Section D, the coupled simulation predicts a significantly lower (-11.5%) foredune deposition compared to the AeoliS-only simulation.

Although the deviations between the results for the different sections appear to be relatively small, they do increase over time, illustrated by the blue and orange bars in Fig. 9d-g and Table 1. These evolving differences between the coupled and AeoliS-only simulations indicate a cumulative effect of marine-aeolian interactions on foredune development. In Section B, the increase in foredune deposition due to the inclusion marine-driven morphodynamics increased from 1.3% in year 1 to 6.7% in year 5. Similarly, the reduction in foredune deposition in Section D increased from -2.4% in year 1 to -24.4% in year 5.

One of the largest deviations between the coupled and AeoliS-only simulations is found at the location with the smallest dune growth along the entire domain (section D, $x \approx 2500 \text{ m}$). While the difference between the AeoliS-only and coupled simulation at this location was relatively small after the first year (-4.2%), after year five, the coupled simulation predicted 48.5% lower dune growth ($5.9 \text{ m}^3/\text{m}/\text{year}$) compared to the AeoliS-only simulation ($11.4 \text{ m}^3/\text{m}/\text{year}$). This finding not only shows the importance of the progressive nature of aeolian-marine interactions but also underscores that the importance of incorporating marine-aeolian interactions in numerical models can be very site-specific.

In summary, although the model shows to be able to reproduce some longshore patterns, it underestimated the magnitude of the longshore variability in both accretive and erosive conditions. This is finally illustrated by comparing the dune growth along the accretive section B and sheltered section D. At section B, characterized by a growing beach and a surplus of sediment supply, foredune growth is observed to be 95% higher than at section D, where the beach has become narrower and is prone to sheltering from the developing spit. While the AeoliS-only model does predict higher dune growth at section B compared to section D (+19%), the coupled model showed a more pronounced difference at 30%. As the Sand Engine continues to evolve, this discrepancy in dune growth becomes larger. After the fifth year, a difference of 219% between sections B and D is observed, compared to simulated differences of 16% and 64% by the AeoliS-only and coupled simulation, respectively.

The modelled impact of both aeolian and marine interactions on the integrated morphodynamics of the Sand Engine, and how developments in one domain affect the other, is summarized in Fig. 10.

4. Discussion

4.1. Advancements in numerical model coupling capabilities

Both wind and wave processes drive sediment transport in many coastal environments and can collectively be critical to their development at a broad range of time scales (storms to centuries) (e.g., Pellón et al., 2020; Garzon et al., 2022; Bauer and Davidson-Arnott, 2003; Ruessink et al., 2022). The interaction of marine and aeolian processes

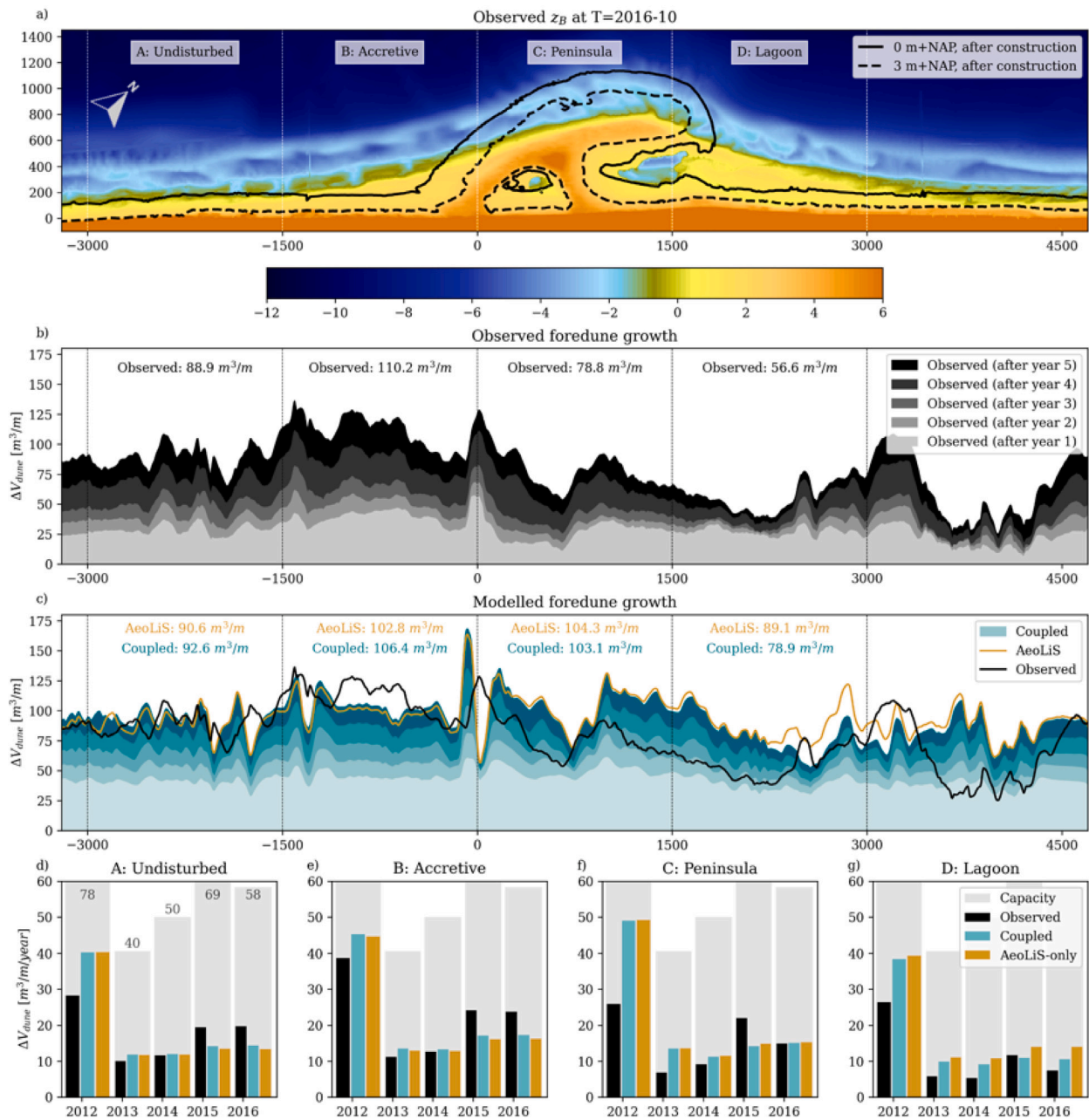


Fig. 9. (a) The bed level after the 10-year evaluation period and initial position of the Sand Engine indicated with contours. (b) The measured and (c) simulated longshore foredune deposition using the coupled model (blue), with yearly growth indicated by varying colour saturation. The foredune depositions after 5 years, as observed (black) and computed by AeoliS-only (orange), are added for comparison. (d–g) Yearly growth rates for sections A–D computed for wind-driven capacity (grey), observations (black), coupled model results (blue) and AeoliS-only results (orange).

Table 1

Relative contribution (%) of including marine-driven morphodynamics in the coupled modelling for the predicted foredune deposition volumes in Sectors A–D during years 1 to 5.

Section	Year					Total
	1	2	3	4	5	
A	-0.1	+1.0	+1.8	+5.7	+7.5	+2.3%
B	+1.3	+4.5	+3.2	+5.9	+6.7	+3.5%
C	-0.4	-0.3	-2.1	-4.4	-0.9	-1.2%
D	-2.4	-10.7	-15.1	-22.0	-24.4	-11.5%

in part contributes to complex, alongshore varying evolution of coastal dunes (e.g., Psuty, 2008; Cohn et al., 2018). This connectivity between

the marine domain and the growth rates or geomorphic characteristics of aeolian landforms has long been recognized through conceptual models (Houser, 2009; Pellón et al., 2020; Sherman and Bauer, 1993; Psuty, 2008; Short and Hesp, 1982), however our reliance on (often limited) long-term morphologic observations limits the transferability of trends yielded from conceptual models into predictive capabilities. Accurately forecasting coastal evolution, including the height of coastal foredunes, is critically important for quantifying present and future coastal risk.

To this point, numerical applications of coastal change in response have typically either focused exclusively on marine (e.g., Lesser et al., 2004) or aeolian (e.g., Hoonhout and de Vries, 2016; Durán and Moore, 2013) processes independently to forecast erosional or accretional dynamics across the coastal profile. Recent developments have

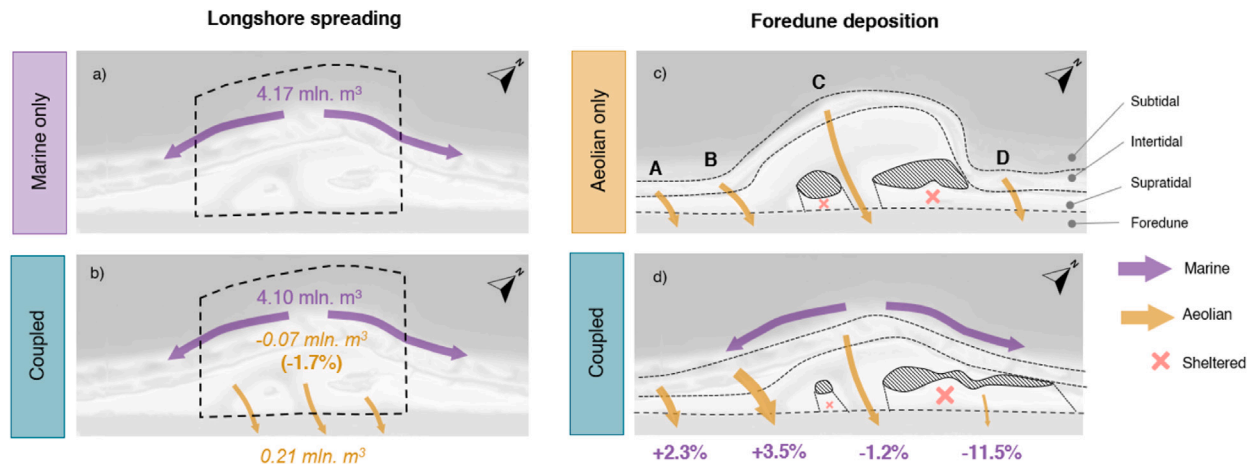


Fig. 10. Visual representation of the impact of interactions between aeolian and marine morphodynamics on longshore dispersion (left) and foredune deposition (right) in uncoupled (upper) and coupled (lower) situations. Comparing the marine-driven longshore dispersion without (a) and with (b) aeolian-driven development shows aeolian transport from beach to dune to cause a reduction in marine-driven longshore dispersion (−1.7%). The impact of marine-driven morphodynamics on aeolian-driven foredune deposition is shown by comparing the AeoliS-only (c) and coupled (d) situations. Marine-driven morphodynamics result in accretion south of the Sand Engine (section B), coinciding with a local increase in foredune deposition (+3.5%), while northern spit development (section C) causes a local decrease in dune growth due to sheltering against waves (−11.5%).

also resulted in the coupling of models for simulating comprehensive 1D profile changes that incorporate both marine and aeolian effects on a range of timescales (e.g., Roelvink and Costas, 2019; Cohn et al., 2019; Ciarletta et al., 2019). While these 1D approaches provide an important step forward in both predictive technology of coastal profile change across the land–water interface and improved understanding of aeolian-marine feedback mechanisms, one-dimensional approaches require an assumption that alongshore variability in both forcing and response is negligible. This assumption is likely suitable for locations with wide flat beaches and long, continuous foredune ridges. Assumptions of longshore uniformity may have more limitations in sites with more spatially complex beach or dune morphology.

Only limited applications have expanded beyond the 1D characterization of coupled aeolian-marine systems. For example, Durán and Moore (2015) added capabilities into the aeolian Coastal Dune Model to additionally empirically assess wave-driven morphology change. However, the cross-shore only implementation of the wind solver in the model setup primarily focused on exploring the general behaviour of coastal systems moreso than the ability to hindcast specific wind and wave events. The cellular automata model of DUBEVEG uses a rule-based and probabilistic approach to modelling the general behaviour of beach, dune, and vegetation dynamics in 2D as well (Keijsers et al., 2016). However, this tool does not simulate underwater sediment transport and, therefore, perhaps neglects exchanges of sediment across the land–water interface and the resultant implications for sediment availability for wind-blown mobilization. These various 1D and 2D tools all provide a valuable framework for advancing knowledge on nearshore–beach–dune interactions and potentially improving predictive skills for simulating coastal change hazards. However, only a fully 2D or 3D modelling framework can be used to assess (1) direct linkages of beach nourishment and its diffusion with time on long-term dune growth rates, (2) the role of spatially complex water bodies on sediment dynamics, and (3) the design of two-dimensional NBS.

The coupled model presented in this study shows the potential to describe the integrated spatiotemporal development of the nearshore–beach–dune system quantitatively on complex coastal landforms. This is achieved by facilitating the concurrent simulation of aeolian and marine development and integrating supply limitations based on dynamically changing conditions. Within a single framework, the ability to simulate marine redistribution of a mega nourishment through alongshore and cross-shore processes, tidal dynamics within a lagoonal setting and corresponding constraints on sediment availability, and armouring-related effects on wind-driven sediment transport are all

demonstrated given confidence in the framework’s ability to resolve the relevant morphodynamics of the system. As demonstrated, the presence of open coast and enclosed water bodies within the model domain imposes important implications on spatial patterns for both sediment mobilization and deposition, with the model successfully able to reproduce shadowing and supply effects of these water bodies on landward sediment fluxes into the dune (Fig. 9a–b). One-dimensional tools could not effectively resolve such spatially complex trends. The relevance of integrating morphodynamics is proven by the increasing impact of marine transport on aeolian development (Fig. 10) and aeolian transport on marine development (Table 1) over time. As the system evolves, so do the geomorphological characteristics that regulate aeolian and marine transport including beach widths and slopes. Both the impact of the accretive intertidal area on aeolian sediment availability and the sheltering effect of the evolving tidal channel (Fig. 10d) could not have been depicted by static fetch-based approaches (Houser, 2009; Pellón et al., 2020). As such, as Sand Engine concept designs (Johnson et al., 2020; Boskalis, 2022) and other NBS (Arens et al., 2013a; Gerhardt-Smith et al., 2015; Steetzel et al., 2017; Osswald et al., 2019; Kroon et al., 2022) are being considered globally for cost-effectively protecting large coastal stretches through leveraging natural processes, the need to utilize appropriate 2D numerical frameworks to support cost justifications and to quantify benefits is encouraged.

However, these advancements are not without their drawbacks. Our attempt to provide a comprehensive, process-based depiction of the nearshore–beach–dune evolution exposed limitations in our understanding and modelling capabilities of the inter- and supratidal zones, as shown by the underpredicted bed level elevation of the beach in Fig. 5. Simpler approaches allow for assumptions that reduce complexity and subsequent computational costs. Suppose one is primarily interested in aeolian development. Would the slight increase in realism justify the five-fold increase in computational time necessitated by including marine-driven morphodynamics (Section 2.5.3)? These additional computational costs also result in more difficulties for efficient model calibration. Moreover, a complex coupled modelling approach introduces new technical challenges. Including increasingly more sophisticated models can lead to an increase in instabilities and errors, exponentially complicating error resolution as potential error sources multiply.

Lastly, we acknowledge that our results do not necessarily indicate a general improvement in predictive skill when using comprehensive coupling methods. The successful prediction of both aeolian and marine domains (Fig. 6) can largely be attributed to the advantages

of having two well-calibrated standalone models (Luijendijk et al., 2017; Hoonhout and de Vries, 2019), backed by an extensive dataset from the Sand Engine (Roest et al., 2021). Despite that, there are still missing physical processes in all of these tools, including direct simulation of groundwater effects, lack of infragravity processes on swash zone sediment transport and hydrodynamics, and simplification of eco-morphodynamic effects, which limit the ability to synthesize all of the dominant physical factors driving coastal change. Additionally, it is well recognized that even with an adequately calibrated model, model physics does not represent all complex eco-morphodynamic effects in coastal systems. Increasing complexity also does not necessarily translate into more accurate predictions (Salt, 2008). Thus, while coupled modelling frameworks serve as a tool for understanding system behaviour, model assumptions, lacking physics, and inherent limitations of models must be recognized in interpreting the results. The tradeoffs between model fidelity and computational grid sizes were chosen here specifically to simulate multi-year periods in a reasonable duration (e.g., weeks) with the ability to successfully simulate the primary drivers and controls on sediment transport across the land–water interface and into the dune. With the tool, we did show that the evolving interactions between aeolian and marine processes affect the complicated integrated development of NBS. The ability to simulate these complex 2D dynamics represents a step forward in capability that did not previously exist.

Deviations between field observations and model results in this study may underexpose the impact of the studied domain interactions on the integrated development. Still, they should not detract from the potential necessity of including domain interactions in future studies. We anticipate that including processes related to groundwater, meteorology, and swash could improve accurately simulating the supratidal domain. Additionally, these processes could also be necessary for the simulation of more complex aeolian landforms, such as blowouts (Hesp, 2002; Ruessink et al., 2018; van Kuik et al., 2022), embryonal dunes (van Puijenbroek et al., 2017), or foredune dynamics (Moore et al., 2016), although it would require a more realistic description of vegetation dynamics (Durán and Moore, 2013); e.g. the relation of vegetation growth to sediment burial (Nolet et al., 2018). Future research should focus more on identifying coastal scenarios where these sophisticated coupled methods could add value and determining which processes should be included.

4.2. Interactions between marine and aeolian processes

Many studies have demonstrated that the concurrent evolution of nearshore–beach–dune systems is sculpted by both marine and aeolian processes (Short and Hesp, 1982; Sherman and Bauer, 1993; Bauer and Davidson-Arnott, 2003; Aagaard et al., 2004; Houser, 2009; Silva et al., 2019; Hallin et al., 2019a; Costas et al., 2020; Pellón et al., 2020; González-Villanueva et al., 2023). Many of these studies, while informed by field data, are largely conceptual, given the complexity of linking above and below-water processes. As such, more commonly, studies and models have traditionally focused on discrete compartments of the coastal tract, such as the nearshore, beach, or dune. However, the advancement of comprehensive numerical tools, such as the presented Delft3D-SWAN-AeoLis coupling framework, provides a tool to further understand and explore these interactions across the land–water divide.

In this study, we focus on assessing the impact of subaerial developments on the subaqueous domain, and vice versa. The former is assessed by quantifying the impact of aeolian processes on marine-driven longshore dispersion, and the latter by estimating the influence of marine-driven morphodynamics on longshore variability in dune growth.

During the Sand Engine's initial design phase, aeolian processes were not taken into account, completely ignoring the subaerial domain Mulder and Tonnon (2011). Throughout the 5-year evaluation

period, significant subaerial landform development was observed and in total 214,000 m³ of sediment was transported into the dunes along the peninsula-domain, as depicted in Fig. 10. Over the Sand Engine's projected lifespan of more than 20 years, this volume can amount to at least 1.5 Mm³, considering the observed dune growth along the domain ($\approx 15 \text{ m}^3/\text{m}/\text{year}$) and its expanding longshore dimension ($> 5 \text{ km}$) (Huisman et al., 2021). Considering that this volume is equivalent to a substantial Dutch shoreface nourishment (Brand et al., 2022), it is reasonable to anticipate that subtracting such volume from the sediment budget would have a significant impact on the Sand Engine's, marine-driven, longshore dispersion.

Comparing the Delft3D-FM-only and coupled simulations enabled us to estimate the actual magnitude of aeolian processes on longshore spreading, which showed only a modest 1.7% reduction in volumetric erosion. Note that this result should be seen in the light of the (very) large longshore transport gradients as a result of the Sand Engine's construction. In such an extreme scenario, the relative impact of aeolian processes may appear minor, but in less dynamic interventions, aeolian transport to the dunes may play a more substantial role. For timescales beyond the 5 years assessed in this study, consistent aeolian sediment transport to the dunes (de Vries et al., 2012) will continue re-allocation of sediment from the intertidal and beach regions to regions further landward. This large sediment redistribution in turn has a feedback on the marine dynamics that could reduce the long term effectiveness of the Sand Motor for its downdrift sediment delivery and associated flood protection services that longshore sediment transport driven beach growth is expected to provide. Finally, the computed decrease in longshore dispersion accounted for only 33% of the volume deposited in the dunes, partly because large amounts of sand were initially eroded from the supratidal beachface, not directly affecting the marine sediment balance. However, while the Sand Engine's shoreline will keep migrating onshore, erosion from the subaerial domain will eventually start to affect the volume of the onshore shifting subaqueous domain.

Similarly, we evaluated the impact of nearshore morphodynamics on the longshore variability in foredune growth. Past research has emphasized the critical role of marine supply in maintaining sediment availability for aeolian transport (Houser, 2009; Cohn et al., 2018; Pellón et al., 2020). Informed by the previously documented evolution of the Sand Engine via alongshore redistribution of sediment (de Schipper et al., 2016; Roest et al., 2021), we expected a substantial positive influence on foredune deposition along the southern flank of the Sand Engine (Fig. 10). The available field observations partially affirmed this prediction, as volume changes increased in the main portion of the Sand Engine relative to the undisturbed region (A \rightarrow B: +24%, Fig. 9b).

Additionally, given a proposed relationship between foredune size and incoming wave energy (Moulton et al., 2021), in addition to the critical role of the intertidal domain as a source for aeolian pickup (Hoonhout and de Vries, 2017; Bauer et al., 2009), we anticipated the tidal channel north of the lagoon to contribute to reduced local foredune deposition. The formation of this tidal channel effectively disconnected the intertidal domain from the foredune, providing the landward beach increased shelter from oncoming waves. This sheltering effect minimizes the mixing frequency in the bed's top layer, leading to an increased impact of sediment sorting and armouring on sediment availability for aeolian transport. These expectations were again confirmed by the available field measurements, in which a decrease in foredune deposition was observed behind the tidal channel (A \rightarrow D: -6%, Fig. 9b).

By comparing the AeoLiS-only and coupled model results, we aimed to estimate the influence of marine-driven morphodynamics on foredune deposition quantitatively. Comparative analysis revealed a slight increase (+3.5%) in foredune deposition along the accretive region (Section B in Fig. 9d). And behind the tidal channel, the model indeed predicted a reduction in foredune deposition as a result of marine-driven morphodynamics (-11.5%).

Although the coupled simulation only partially reproduces the observed longshore variability in dune growth (e.g., the difference between sections B and D), it has demonstrated its ability to replicate certain effects of nearshore morphological developments on dune growth. We expect that the model's inability to fully explain the observed longshore variability can be largely attributed to the model not being tailored to describe the integrated development of the nearshore–dune system, but rather to accurately depict both individual domains.

We do suspect that a better representation of the intertidal development in our model (i.e. the deviations illustrated in Fig. 5) will result in a higher predictive accuracy of the alongshore and annual variability in foredune deposition, probably affecting the modelled aeolian-marine interactions. Despite the seeming importance of the intertidal zone in connecting the nearshore to the dunes, numerous processes that shape these zones are not included in this study. The intertidal, or swash, zone has a significant role in connecting the aeolian and marine domain Roelvink and Otero (2017) and Chen et al. (2023), e.g. by transporting sediment from the nearshore to the upper beach during accretive conditions or beach recovery (Hine, 1979; Phillips et al., 2019). As swash morphodynamics are not included in our model description (van Rijn et al., 2011), the maximum elevation of marine-driven accretion is only 2.2 m+NAP (Fig. 5c), much lower than the maximum total water level elevation at the site (van Bemmelen et al., 2020). This underscores the model's limited capacity to deposit sediment higher up into the beach profile, which is supported by the underpredicted bed level elevations in the upper swash zone ($y < 200$ m in Fig. 5b). Swash-driven growth of the beachface could be vital in connecting nearshore sedimentation and aeolian-driven dune growth (Roelvink and Otero, 2017; Chen et al., 2023). The lack of swash-related processes could therefore be a reasonable explanation for the model's inability to fully reproduce the enhanced dune growth along accretive beaches, in this case mainly Section B.

Furthermore, in both simulations, a considerable amount of sediment was available for aeolian transport in the first year, as desert pavements need time to develop. This contrasts with Sand Engine's construction period, which spanned several months, potentially allowing for some degree of armouring before our simulation's starting point. Additionally, a uniform wind field is assumed, while shear perturbations (Kroy et al., 2002; Durán et al., 2010), or boundary layer formation, are found to shape the upper beach profile by reducing velocities towards dunes (Bauer et al., 2009). Observations show a relatively stable upper beach, while the model predicts erosion from the supratidal area ($20 \text{ m} < y < 100$ m in Fig. 5b). Consequently, during the first year, the supratidal zone temporarily served as a sediment source for aeolian transport, stimulating foredune growth in actual sediment-scarce sections (Fig. 9f,g). These limitations are expected to strongly contribute to the overprediction of dune growth during the first year, distorting the comparative analysis between the coupled and AeoliS-only simulations. Solving these model limitations could see a more accurate estimate of the impact of including aeolian-marine interactions in coupled modelling.

While the magnitude of the simulated feedback is relatively small (<15%) for the Sand Engine case study (Fig. 9c), and probably underpredicted due to the described missing processes shaping the beach profile, the Sand Engine and other feeder nourishments are designed to provide benefits over the scale of decades. Aggregating flux modifications over these long timescales can drastically alter the total volume change and form of dune development. The 5-year evaluation period is short relative to the cumulative nature of the evaluated process interactions and dune-building timescales. Given the aggregating nature of the impacts evaluated, it might be beneficial to extend the evaluation period to improve the quantification of their impact. These improvements also necessitate enhancing the framework's scalability, efficiency, and robustness. The spatio-temporal scale, two-dimensionality and high resolution of the presented nearshore–dune simulation are unprecedented.

Despite this, the 5-year period is still relatively short compared to long-term morphological developments shaping the Sand Engine over its lifetime, potentially underexposing the importance of the impact that aeolian processes have on marine developments, and vice versa.

The Sand Engine case also represents a wide coastal beach setting with a large source area for aeolian transport and fewer sediment supply limitations than a narrow beach system with similar grain size attributes. It may be expected that there are other morphodynamic systems where simultaneous simulation of marine and aeolian is more critical to simulate long-term coastal behaviour effectively.

In light of the aforementioned study limitations, evaluating the predictive skill of our approach is further complicated by the fact that the original stand-alone setups were specifically calibrated to align with observed morphodynamics. If the Delft3D-FM model component initially underpredicted longshore spreading, introducing aeolian-driven erosion from the intertidal area as an added factor limits sediment availability for longshore transport even further. This change reduces predictive accuracy, yet we believe it enhances the representation of the physical system. Conversely, if the AeoliS model overpredicted foredune growth, adding marine-driven sediment supply would increase dune growth, potentially lowering the predictive score. Even though, in this study, including nearshore morphodynamics improved foredune predictions across all sections (e.g., for section B, AeoliS-only: -6.7%, coupled: -3.5%; for section D, AeoliS-only: +57.6%, coupled: +39.5%), these results are contingent on the original accuracy of the stand-alone models.

As stated by Barbour and Krahn (2004), the added value of numerical models is not limited to making predictions. Even though, in the context of the current study, both the impact of including aeolian-marine interactions and the improvement in predictive skill are minor, the fact that the coupled model has shown how aeolian processes can impact marine-driven longshore spreading and how nearshore morphodynamics can affect dune growth, the study has provided new insight into the integrated development of nearshore–dune systems. As initial predictions during the Sand Engine's design anticipated a significant increase in dune growth as a result of a large amount of nourished sediment, this study shows that the intricate interactions between marine and aeolian processes cause a much more complicated morphodynamic response of the nearshore–dune system.

5. Conclusions

In this study, we have quantified the impact of interactions between aeolian and marine morphodynamics on the nearshore–dune system. An intercomparison of numerical model simulations has shown the reduction of marine-driven longshore spreading as a result of aeolian fluxes towards the dunes, enhanced dune growth corresponding with nearshore sedimentation, and reduced dune growth along an eroding, sheltered beach. These findings align well with the available bathymetric and topographic measurements and our general system understanding based on existing literature on nearshore–dune dynamics. These findings can help increase the comprehensive understanding of the development of sandy Nature-based Solutions (NBS).

For this purpose, a novel coupling framework was presented that enables a continuous exchange (i.e. frequently during the simulation) of wave heights, bed-, and water levels between three model components: Delft3D Flexible Mesh (Delft3D-FM), SWAN and AeoliS. This coupled model is then applied to simulate the first 5-year development of the Sand Engine: A large mega-nourishment constructed in the Netherlands.

The coupled model results show a concurrent development of the marine zone and the aeolian zone. The former is dominated by lateral dispersion of sand by marine processes with large quantities of sediment being eroded from the peninsula and deposition at the two

adjacent beaches. The aeolian evolution is characterized by a growth of the foredune of $O 15 \text{ m}^3$ per meter alongshore per year. This foredune growth varies in the alongshore as beach properties vary and artificial waterbodies acted as a sediment trap. The coupled model is able to reproduce the main volumetric changes well; i.e. less than 5% deviation of the erosion on the main peninsula (observed: 3.9 Mm^3 , modelled: 4.1 Mm^3). The infilling of the artificial dune lake shows that the model can reproduce the aeolian sediment fluxes with an error in the volumetric change of 15%.

To enable the quantification the impact of aeolian and marine process interactions on the Sand Engine's integrated morphological development, the coupled and uncoupled (i.e. stand-alone) model results were compared. Our model results show that a persistent extraction of material by aeolian transport ($\approx 15 \text{ m}^3/\text{m}/\text{year}$) affects marine sediment transports. The relative impact of the aeolian component is small ($< 5\%$) in the Sand Engine case. The last years in the simulations show a growing relative impact by the aeolian processes suggesting that the landward transport by aeolian transports cannot be ignored when assessing long-term alongshore sediment transport in the marine domain.

The variability in dune growth along the coast is likely influenced significantly by nearshore morphodynamics. At the southern end of the peninsula, which is characterized by marine-driven sedimentation, observed dune growth was 95% higher compared to the section that contains lagoon, spit and channel dynamics where the subaerial beach is small. The incorporation of marine-driven processes in the simulation indeed showed that the developing nearshore morphology impacts the foredune growth over time, leading to a decrease in average dune growth of -24.4% in the fifth year onshore of the lagoon, with maximum up to -48.5% at the most sheltered location. The large observed difference between the accretive part of the beach and lagoon/spit area was partially reproduced by the coupled model at a 30% difference, compared to a 19% difference in the stand-alone simulation, in which nearshore morphodynamics was not included.

This research represents a step towards an integrated approach in the numerical modelling of highly complex nearshore-beach-dune systems. Our first case study demonstrates the impact of including aeolian-marine interactions in the initial response phase of a large-scale Nature-based Solution, highlighting both the value of coupled numerical modelling and yielding new insights on marine-aeolian interactions on inter-annual coastal landform evolution. This newly demonstrated capability and approach opens the door to integrated landform modelling for a broad range of potential spatial (meters to 10 s of kilometers) and temporal scales (hours to decades) in coastal systems where both winds and waves play an active role in sediment transport and net landscape change.

Software availability

The AeoliS model (v2.1.1) (Hoonhout and de Vries, 2016) is an open-source model available under GNU General Public License v3.0 at <https://github.com/openearth/aeolis-python>. The hydrodynamic module of the AeoliS code is locally modified to correctly interpret the exchange of wave properties and water levels from the Delft3D Flexible Mesh model.

The Delft3D Flexible Mesh software (Lesser et al., 2004; Kernkamp et al., 2011, 2023.01 release, SVN revision 76916; October 7, 2022; DIMRset 2.21.17) is available at www.deltares.nl/en/software/delft3d-flexible-mesh-suite/.

The coupling script is written in Python. We aim to publicly release the code after improving the code's robustness, readability, and applicability. Until then, the coupling script and modified AeoliS code are available upon reasonable request.

CRediT authorship contribution statement

Bart van Westen: Conceptualization, Formal analysis, Investigation, Methodology, Software, Validation, Visualization, Writing – original draft. **Arjen P. Luijendijk:** Conceptualization, Funding acquisition, Methodology, Supervision, Writing – review & editing. **Sierd de Vries:** Conceptualization, Funding acquisition, Writing – review & editing. **Nicholas Cohn:** Methodology, Writing – review & editing. **Tim W.B. Leijnse:** Software, Writing – review & editing. **Matthieu A. de Schipper:** Conceptualization, Funding acquisition, Supervision, Writing – review & editing.

Declaration of competing interest

The authors declare that they have no known competing financial interests or personal relationships that could have appeared to influence the work reported in this paper.

Data availability

The morphological data used in this study are openly available at the 4TU.Centre for Research Data: <https://doi.org/10.4121/collection:zandmotor>.

Acknowledgements

This work was supported by the project TKI Dutch Coastline Challenge, The Netherlands, which is co-funded by the Rijksdienst voor Ondernemend Nederland (RVO), The Netherlands, the Dutch Ministry of Infrastructure and Water, The Netherlands, Rijkswaterstaat, The Netherlands, Vereniging van Waterbouwers, The Netherlands, EcoShape, The Netherlands, TU Delft, The Netherlands and the Deltares Strategic Research Program Seas and Coastal Zones, The Netherlands. Their contributions to this research are highly appreciated. The development of the coupling framework is partially funded by the Deltares Strategic Research Programme 'Seas and Coastal Zones', The Netherlands. Furthermore, this work is part of the research programme DuneForce with project number 17064, which is partly financed by the Dutch Research Council (NWO), The Netherlands. Field data was collected by the Dutch Ministry of Infrastructure and the Environment (Rijkswaterstaat) with the support of the Province of South-Holland, the European Fund for Regional Development EFRO and EcoShape Building with Nature. The constructive comments of Stefan Aarninkhof and Peter Herman (Delft University of Technology) helped to shape this study.

Appendix A. Data description and post-processing

For this study, we have reconstructed the 5-year morphodynamic development of the Sand Engine using four bathymetric and topographic datasets: *Sand Engine*, *Nemo*, *JarKuS*, and *LiDAR* surveys by Rijkswaterstaat. All datasets are obtained from Rijkswaterstaat et al. (2016). The spatial coverage of each dataset is depicted in Fig. A.1b and detailed in Table A.1a. In-depth information on these datasets and the Sand Engine's subaqueous development over five years is available in Roest et al. (2021).

We have chosen an analysis domain spanning 15 km alongshore and 2.5 km cross-shore, as outlined in black in Fig. A.1b and c. A local coordinate system similar to that in de Schipper et al. (2016) was used, originating at the 'Schelpenpad' beach entrance (x_{RD} : 72421.9 m, y_{RD} : 451326.1 m), and rotated 48 degrees to create a shore-orthogonal grid. All datasets are interpolated onto a 5 m x 5 m grid using linear interpolation.

For the general model-data comparison (Figs. 4 and 8) and sediment budget analysis (Fig. 6), we merged all datasets into a composite DEMs (Table A.1b). The *Sand Engine* data predominantly covers the

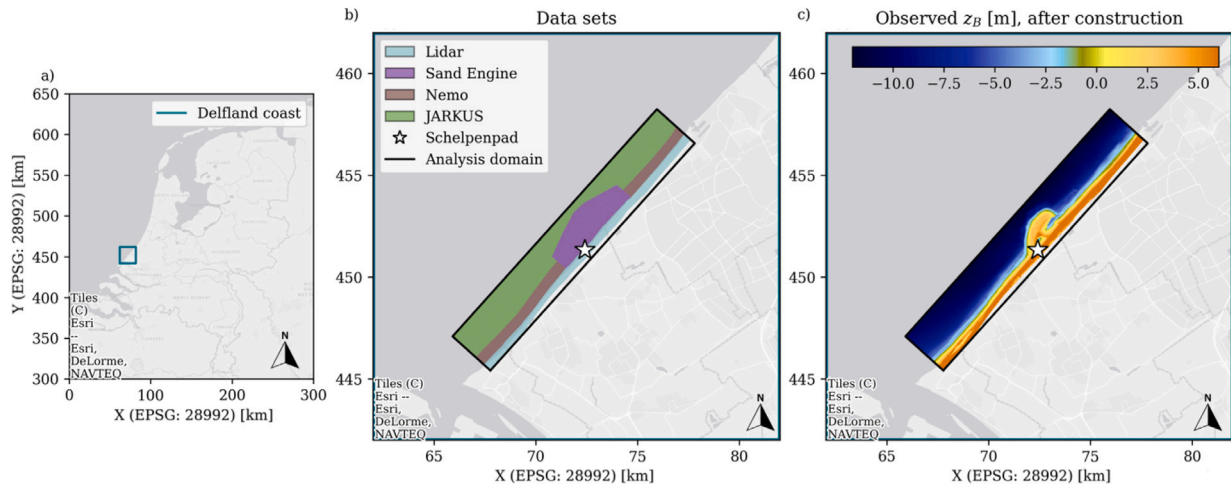


Fig. A.1. (a) Location of the Delfland coast (blue), (b) Overview of the Delfland coast displaying the various datasets utilized in this study. The schelpenpad beach entrance (star symbol) is used as the origin of the shore-orthogonal coordinate system used in the analyses, (c) bed level z_B [m] for the composite DEM directly after construction.

assigned analysis domain (Fig. 6). Where data are missing, they are supplemented with the most recent *Nemo* or *JarKus* data. The *LiDAR* dataset, used only landwards of the analysis domain, does not affect these results (Fig. A.1b). We applied smoothing around the transitions between the *Nemo* and *Sand Engine* datasets to maintain realistic transition gradients. Additionally, a temporary sand stockpile present after construction, and subsequently removed by machinery (19,000 m³, 220 m in length, alongshore density of 86 m³/m), is filtered out of the topography.

The coupled model provides weekly outputs, and the closest output moment to each comparison in time is chosen based on the survey date of the *Sand Engine* dataset, which is generally conducted during calm periods. As such, the influence of morphological differences between datasets with differing survey dates is likely to be minimal. The most significant deviation between reference and survey dates is in the *JarKus* data. However, as this data is used only to fill the stable offshore portion of the domain, its impact is deemed insignificant.

For the foredune deposition analysis specifically, we solely utilize the *LiDAR* dataset (Table A.1c), minimizing deviations between model and measurement dates.

Appendix B. Theoretical potential dune growth

The potential aeolian-driven transport capacity Q_{pot} [kg/s] ($= f(u_*, u_{th})$) is computed to serve as a proxy for the relative importance of the prevailing environmental conditions. The transport capacity is calculated using the default transport equation in Aeolis (Bagnold, 1937). The input shear velocity u_* [m/s] is based on the wind forcing in Aeolis and the velocity threshold u_{th} [m/s] is determined with the most prevalent grain size ($= 354 \mu\text{m}$). The transport rate is converted to potential dune volume growth per running meter to enable comparison with measured dune growth (Hoonhout and de Vries, 2019):

$$\Delta V_{pot} = \frac{Q_{pot} f_{\theta,os} \Delta T}{(1-p)\rho_{grain}} \tag{B.1}$$

Potential dune growth ΔV_{pot} [m³/m] is computed by integrating over time (ΔT), converting from mass to volume based on porosity p ($=0.4$) and grain density ρ_g ($=2650 \text{ kg/m}^3$), and considering only the onshore wind directions (θ_u):

$$f_{\theta,os} = \max(0; \cos 312^\circ - \theta_u) \tag{B.2}$$

Table A.1

Overview of datasets used for the Sand Engine’s morphodynamic reconstruction. (a) The dataset’s coverage, resolution, and survey count. (b) Dates and corresponding survey numbers (in brackets), used for the visual comparison (Fig. 4 and Fig. 8), and sediment balance analysis (Fig. 6). (c) The dates related to the foredune deposition analysis (Fig. 9).

(a) Spatiotemporal coverage				
	Lidar	Sand Engine	Nemo	JarKus
Resolution	2 m × 2 m	40 m × 5 m	25 m × 5 m	250 m × 5 m
Number of surveys	19	52	21	12
(b) Composite DEMs. Dates (survey numbers). Used for Visual comparison (Figs. 4 & 8) and Sediment balance (Fig. 6)				
	Lidar	Sand Engine	Nemo	JarKus
Initial	11/07/2011 (2)	02/08/2011 (2)	JarKus	15/02/2011 (1)
After 5 years	15/02/2016 (11)	06/07/2016 (37)	07/05/2016 (19)	20/04/2015 (5)
(c) Dates (survey numbers) : Foredune deposition (Fig. 9)				
	Lidar	Sand Engine	Nemo	JarKus
Initial	11/07/2011 (2)			
After 1 year	08/10/2012 (4)			
After 2 years	01/10/2013 (6)			Not used
After 3 years	03/10/2014 (8)			
After 4 years	01/10/2015 (10)			
After 5 years	05/10/2016 (12)			

References

- Aagaard, T., Davidson-Arnott, R., Greenwood, B., Nielsen, J., 2004. Sediment supply from shoreface to dunes: Linking sediment transport measurements and long-term morphological evolution. *Geomorphology* 60, 205–224. <http://dx.doi.org/10.1016/j.geomorph.2003.08.002>.
- Arens, S.M., Mulder, J.P., Slings, Q.L., Geelen, L.H., Damsma, P., 2013a. Dynamic dune management, integrating objectives of nature development and coastal safety: Examples from the Netherlands. *Geomorphology* 199, 205–213.
- Arens, S.M., Slings, Q.L., Geelen, L.H., Van der Hagen, H.G., 2013b. Restoration of dune mobility in the Netherlands. In: *Restoration of Coastal Dunes*. Springer, pp. 107–124.
- Bagnold, R.A., 1937. The transport of sand by wind. *Geogr. J.* 89 (5), 409–438.
- Barbour, S.L., Krahn, J., 2004. Numerical modelling—prediction or process. *Geotech. News* 22 (4), 44–52.
- Barciela Rial, M., 2019. Consolidation and drying of slurries: A building with nature study for the marker wadden (Ph.D. thesis). Delft University of Technology.
- Bauer, B.O., Davidson-Arnott, R.G., 2003. A general framework for modeling sediment supply to coastal dunes including wind angle, beach geometry, and fetch effects. *Geomorphology* 49 (1–2), 89–108.
- Bauer, B.O., Davidson-Arnott, R.G., Hesp, P.A., Namikas, S.L., Ollerhead, J., Walker, I.J., 2009. Aeolian sediment transport on a beach: Surface moisture, wind fetch, and mean transport. *Geomorphology* 105, 106–116. <http://dx.doi.org/10.1016/j.geomorph.2008.02.016>.
- Booij, N., Ris, R.C., Holthuijsen, L.H., 1999. A third-generation wave model for coastal regions: 1. Model description and validation. *J. Geophys. Res.: Oceans* 104 (C4), 7649–7666.
- Boskalis, 2022. Boskalis to protect eroded togo and benin coastline and construct innovative sand engine concept for beach replenishment. URL <https://boskalis.com/press/press-releases-and-company-news/boskalis-to-protect-eroded-togo-and-benin-coastline-and-construct-innovative-sand-engine-concept-for-beach-replenishment>.
- Brand, E., Ramaekers, G., Lodder, Q., 2022. Dutch experience with sand nourishments for dynamic coastline conservation—an operational overview. *Ocean Coast. Manag.* 217, 106008.
- Bridges, T.S., King, J.K., Simm, J.D., Beck, M.W., Collins, G., Lodder, Q., Mohan, R.K., 2021. Overview: International Guidelines on Natural and Nature-Based Features for Flood Risk Management. Engineer Research and Development Center (US).
- Carter, R., 1976. Formation, maintenance and geomorphological significance of an aeolian shell pavement. *J. Sediment. Res.* 46 (2), 418–429.
- Chen, W., van der Werf, J.J., Hulscher, S.J.M.H., 2023. A review of practical models of sand transport in the swash zone. *Earth-Sci. Rev.* 104355.
- Ciarletta, D.J., Shawler, J.L., Tenebruso, C., Hein, C.J., Lorenzo-Trueba, J., 2019. Re-constructing Coastal sediment budgets from beach- and foredune-ridge morphology: A coupled field and modeling approach. *J. Geophys. Res.: Earth Surf.* 124 (6), 1398–1416. <http://dx.doi.org/10.1029/2018JF004908>.
- Cohn, N., Hoonhout, B.M., Goldstein, E.B., de Vries, S., Moore, L.J., Vinent, O.D., Ruggiero, P., 2019. Exploring marine and aeolian controls on coastal foredune growth using a coupled numerical model. *J. Mar. Sci. Eng.* 7, <http://dx.doi.org/10.3390/jmse7010013>.
- Cohn, N., Ruggiero, P., de Vries, S., García-Medina, G., 2017. Beach growth driven by intertidal sandbar welding. In: *Proceedings of Coastal Dynamics*. Vol. 1, (99), pp. 12–16.
- Cohn, N., Ruggiero, P., de Vries, S., Kaminsky, G.M., 2018. New insights on coastal foredune growth: The relative contributions of marine and aeolian processes. *Geophys. Res. Lett.* 45 (10), 4965–4973.
- Costas, S., de Sousa, L.B., Kombiadou, K., Ferreira, Ó., Plomaritis, T.A., 2020. Exploring foredune growth capacity in a coarse sandy beach. *Geomorphology* 371, 107435.
- de Schipper, M.A., Ludka, B.C., Raubenheimer, B., Luijendijk, A.P., Schlacher, T.A., 2021. Beach nourishment has complex implications for the future of sandy shores. *Nat. Rev. Earth Environ.* 2, 70–84. <http://dx.doi.org/10.1038/s43017-020-00109-9>.
- de Schipper, M.A., de Vries, S., Ruessink, G., de Zeeuw, R.C., Rutten, J., van Gelder-Maas, C., Stive, M.J., 2016. Initial spreading of a mega feeder nourishment: Observations of the Sand Engine pilot project. *Coast. Eng.* 111, 23–38.
- de Vriend, H.J., van Koningsveld, M., Aarninkhof, S.G., de Vries, M.B., Baptist, M.J., 2015. Sustainable hydraulic engineering through building with nature. *J. Hydro-Environ. Res.* 9, 159–171. <http://dx.doi.org/10.1016/j.jher.2014.06.004>.
- de Vriend, H.J., Rijkswaterstaat, Roelvink, J.A., 1989. Innovatie Van Kustverdediging: Inspelen Op Het Kuststelsysteem. Ministerie van Verkeer en Waterstaat.
- de Vries, S., Arens, S., de Schipper, M., Ranasinghe, R., 2014a. Aeolian sediment transport on a beach with a varying sediment supply. *Aeolian Res.* 15, 235–244. <http://dx.doi.org/10.1016/j.aeolia.2014.08.001>.
- de Vries, S., Southgate, H., Kanning, W., Ranasinghe, R., 2012. Dune behavior and aeolian transport on decadal timescales. *Coast. Eng.* 67, 41–53. <http://dx.doi.org/10.1016/j.coastaleng.2012.04.002>.
- de Vries, S., van Thiel de Vries, J., van Rijn, L.C., Arens, S.M., Ranasinghe, R., 2014b. Aeolian sediment transport in supply limited situations. *Aeolian Res.* 12, 75–85. <http://dx.doi.org/10.1016/j.aeolia.2013.11.005>.
- Delgado-Fernandez, I., 2010. A review of the application of the fetch effect to modelling sand supply to coastal foredunes. *Aeolian Res.* 2 (2–3), 61–70.
- Deltares, 1982. Deltares integrated model runner.
- Durán, O., Moore, L.J., 2013. Vegetation controls on the maximum size of coastal dunes. *Proc. Natl. Acad. Sci.* 110 (43), 17217–17222.
- Durán, O., Moore, L.J., 2015. Barrier island bistability induced by biophysical interactions. *Nature Clim. Change* 5 (2), 158–162.
- Durán, O., Parteli, E.J., Herrmann, H.J., 2010. A continuous model for sand dunes: Review, new developments and application to barchan dunes and barchan dune fields. *Earth Surf. Processes Landforms* 35 (13), 1591–1600.
- Garzon, J.L., Costas, S., Ferreira, O., 2022. Biotic and abiotic factors governing dune response to storm events. *Earth Surf. Process. Landforms* 47 (4), 1013–1031.
- Gerhardt-Smith, J.M., McDonald, J.S., Rees, S.I., Lovelace, N.D., et al., 2015. Deer island aquatic ecosystem restoration project.
- González-Villanueva, R., Pastoriza, M., Hernández, A., Carballeira, R., Sáez, A., Bao, R., 2023. Primary drivers of dune cover and shoreline dynamics: A conceptual model based on the Iberian Atlantic coast. *Geomorphology* 423, 108556.
- Hallin, C., Huisman, B.J., Larson, M., Walstra, D.-J.R., Hanson, H., 2019a. Impact of sediment supply on decadal-scale dune evolution—Analysis and modelling of the Kennemer dunes in the Netherlands. *Geomorphology* 337, 94–110.
- Hallin, C., van IJzendoorn, C., Homberger, J.-M., de Vries, S., 2023. Simulating surface soil moisture on sandy beaches. *Coast. Eng.* 104376.
- Hallin, C., Larson, M., Hanson, H., 2019b. Simulating beach and dune evolution at decadal to centennial scale under rising sea levels. *PLoS One* 14 (4), e0215651.
- Hervouet, J.-M., Bates, P., 2000. The telemac modelling system special issue. *Hydrol. Process.* 14 (13), 2207–2208.
- Hesp, P., 2002. Foredunes and blowouts: initiation, geomorphology and dynamics. *Geomorphology* 48 (1–3), 245–268.
- Hine, A.C., 1979. Mechanisms of berm development and resulting beach growth along a barrier spit complex. *Sedimentology* 26 (3), 333–351.
- Hoonhout, B., 2016. Windsurf. <https://github.com/openearth/windsurf>.
- Hoonhout, B.M., de Vries, S., 2016. A process-based model for aeolian sediment transport and spatiotemporal varying sediment availability. *J. Geophys. Res.: Earth Surf.* 121 (8), 1555–1575.
- Hoonhout, B., de Vries, S., 2017. Aeolian sediment supply at a mega nourishment. *Coast. Eng.* 123, 11–20. <http://dx.doi.org/10.1016/j.coastaleng.2017.03.001>.
- Hoonhout, B., de Vries, S., 2019. Simulating spatiotemporal aeolian sediment supply at a mega nourishment. *Coast. Eng.* 145, 21–35.
- Houser, C., 2009. Synchronization of transport and supply in beach-dune interaction. *Progr. Phys. Geogr.* 33, 733–746. <http://dx.doi.org/10.1177/0309133309350120>.
- Hovenga, P.A., Ruggiero, P., Itzkin, M., Jay, K.R., Moore, L., Hacker, S.D., 2023. Quantifying the relative influence of coastal foredune growth factors on the US mid-Atlantic Coast using field observations and the process-based numerical model Windsurf. *Coast. Eng.* 181, 104272.
- Huisman, B., Wijsman, J., Arens, S., Versteeg, C., van der Valk, L., van Donk, S., Vreugdenhil, H., Taal, M., 2021. Evaluatie van 10 jaar zandmotor: Bevindingen uit het monitoring-en evaluatie programma (MEP) voor de periode 2011 tot 2021. Technical Report, Deltares.
- Hutton, E.W., Piper, M.D., Tucker, G.E., 2020. The Basic Model Interface 2.0: A standard interface for coupling numerical models in the geosciences. *J. Open Source Softw.* 5 (51), 2317.
- Johnson, M., Goodliffe, R., Doygun, G., Flikweert, J., 2020. The UK's first sandscaping project (Bacton, Norfolk) from idea to reality. In: *Coastal Management 2019: Joining Forces To Shape Our Future Coasts*. ICE Publishing, pp. 333–345.
- Keijsers, J., De Groot, A., Riksen, M., 2016. Modeling the biogeomorphic evolution of coastal dunes in response to climate change. *J. Geophys. Res.: Earth Surf.* 121 (6), 1161–1181.
- Kernkamp, H.W., Van Dam, A., Stelling, G.S., de Goede, E.D., 2011. Efficient scheme for the shallow water equations on unstructured grids with application to the Continental Shelf. *Ocean Dyn.* 61, 1175–1188.
- Kroon, A., de Schipper, M., de Vries, S., Aarninkhof, S., 2022. Subaqueous and subaerial beach changes after implementation of a mega nourishment in front of a sea dike. *J. Mar. Sci. Eng.* 10 (8), 1152.
- Kroy, K., Sauermaann, G., Herrmann, H.J., 2002. Minimal model for sand dunes. *Phys. Rev. Lett.* 88 (5), 054301.
- Larson, M., Erikson, L., Hanson, H., 2004. An analytical model to predict dune erosion due to wave impact. *Coast. Eng.* 51 (8–9), 675–696.
- Larson, M., Palalane, J., Fredriksson, C., Hanson, H., 2016. Simulating cross-shore material exchange at decadal scale. Theory and model component validation. *Coast. Eng.* 116, 57–66.
- Lesser, G.R., Roelvink, J.A., van Kester, J.A., Stelling, G.S., 2004. Development and validation of a three-dimensional morphological model. *Coast. Eng.* 51 (8–9), 883–915.
- Luijendijk, A., van Oudenhoven, A., 2019. The Sand Motor: A Nature-Based Response to Climate Change: Findings and Reflections of the Interdisciplinary Research Program NatureCoast. Delft University Publishers.
- Luijendijk, A.P., Ranasinghe, R., de Schipper, M.A., Huisman, B.A., Swinkels, C.M., Walstra, D.J., Stive, M.J., 2017. The initial morphological response of the sand engine: A process-based modelling study. *Coast. Eng.* 119, 1–14.

- Luijendijk, A., de Vries, S., van het Hooft, T., de Schipper, M., 2019. Predicting dune growth at the sand engine by coupling the delft3d flexible mesh and aeolis models. In: *Coastal Sediments 2019: Proceedings of the 9th International Conference*. World Scientific, pp. 1319–1326.
- Moore, L.J., Vinent, O.D., Ruggiero, P., 2016. Vegetation control allows autocyclic formation of multiple dunes on prograding coasts. *Geology* 44 (7), 559–562.
- Moulton, M.A., Hesp, P.A., da Silva, G.M., Keane, R., Fernandez, G.B., 2021. Surfzone-beach-dune interactions along a variable low wave energy dissipative beach. *Mar. Geol.* 435, 106438.
- Mulder, J.P., Tonnon, P.K., 2011. Sand engine: background and design of a mega-nourishment pilot in the Netherlands. *Coast. Eng. Proc.* (32), 35.
- Nolet, C., Van Puijenbroek, M., Suomalainen, J., Limpens, J., Riksen, M., 2018. UAV-imaging to model growth response of marram grass to sand burial: Implications for coastal dune development. *Aeolian Res.* 31, 50–61.
- Osswald, F., Dolch, T., Reise, K., 2019. Remobilizing stabilized island dunes for keeping up with sea level rise? *J. Coast. Conserv.* 23 (3), 675–687.
- Palalane, J., Fredriksson, C., Marinho, B., Larson, M., Hanson, H., Coelho, C., 2016. Simulating cross-shore material exchange at decadal scale. *Model application. Coast. Eng.* 116, 26–41.
- Pellón, E., de Almeida, L., González, M., Medina, R., 2020. Relationship between foredune profile morphology and aeolian and marine dynamics: A conceptual model. *Geomorphology* 351, 106984.
- Phillips, M., Blenkinsopp, C., Splinter, K., Harley, M., Turner, I., 2019. Modes of berm and beachface recovery following storm reset: Observations using a continuously scanning lidar. *J. Geophys. Res.: Earth Surf.* 124 (3), 720–736.
- Psuty, N., 2008. The coastal foredune: a morphological basis for regional coastal dune development. In: *Coastal Dunes*. Springer, pp. 11–27.
- Quartel, S., Kroon, A., Ruessink, B., 2008. Seasonal accretion and erosion patterns of a microtidal sandy beach. *Mar. Geol.* 250 (1–2), 19–33.
- Ranasinghe, R., Swinkels, C., Luijendijk, A., Roelvink, D., Bosboom, J., Stive, M., Walstra, D., 2011. Morphodynamic upscaling with the MORFAC approach: Dependencies and sensitivities. *Coast. Eng.* 58 (8), 806–811.
- Rijkswaterstaat, Zuid-Holland, P., EcoShape, 2016. Zandmotor data / sand motor data. <http://dx.doi.org/10.4121/COLLECTION:ZANDMOTOR>, URL https://data.4tu.nl/collections/_/5065412/1.
- Roelvink, D., Costas, S., 2019. Coupling nearshore and aeolian processes: Xbeach and duna process-based models. *Environ. Model. Softw.* 115, 98–112.
- Roelvink, D., Otero, S.C., 2017. Beach berms as an essential link between subaqueous and subaerial beach/dune profiles. *Geotemas (Madrid)* (17), 79–82.
- Roelvink, D., Reniers, A., Van Dongeren, A., De Vries, J.V.T., McCall, R., Lescinski, J., 2009. Modelling storm impacts on beaches, dunes and barrier islands. *Coast. Eng.* 56 (11–12), 1133–1152.
- Roelvink, J., Walstra, D.-J., 2004. Keeping it simple by using complex models. *Adv. Hydro-sci. Eng.* 6, 1–11.
- Roest, B., de Vries, S., de Schipper, M., Aarninkhof, S., 2021. Observed changes of a mega feeder nourishment in a coastal cell: Five years of sand engine morphodynamics. *J. Mar. Sci. Eng.* 9 (1), 37.
- Ruessink, B., Arens, S., Kuipers, M., Donker, J., 2018. Coastal dune dynamics in response to excavated foredune notches. *Aeolian Res.* 31, 3–17.
- Ruessink, G., Sterk, G., Smit, Y., Winter, W.D., Hage, P., Donker, J.J., Arens, S.M., 2022. Predicting monthly to multi-annual foredune growth at a narrow beach. *Earth Surf. Process. Landforms* 47, 1845–1859. <http://dx.doi.org/10.1002/esp.5350>.
- Rutten, J., Ruessink, B., Price, T., 2018. Observations on sandbar behaviour along a man-made curved coast. *Earth Surf. Process. Landforms* 43 (1), 134–149.
- Salt, J.D., 2008. The seven habits of highly defective simulation projects. *J. Simul.* 2, 155–161.
- Sherman, D.J., Bauer, B.O., 1993. Dynamics of beach-dune systems. *Progr. Phys. Geogr.* 17 (4), 413–447.
- Sherman, D.J., Li, B., 2012. Predicting aeolian sand transport rates: A reevaluation of models. *Aeolian Res.* 3 (4), 371–378.
- Short, A.D., Hesp, P.A., 1982. Wave, beach and dune interactions in southeastern Australia. *Mar. Geol.* 48 (3–4), 259–284.
- Silva, F.G., Wijnberg, K.M., de Groot, A.V., Hulscher, S.J., 2019. The effects of beach width variability on coastal dune development at decadal scales. *Geomorphology* 329, 58–69.
- Sørensen, M., 2004. On the rate of aeolian sand transport. *Geomorphology* 59 (1–4), 53–62.
- Steetzel, H., van der Goot, F., Fiselier, J., de Lange, M., Penning, E., van Santen, R., Vuik, V., 2017. Building with nature pilot sandy foreshore houtribdijk design and behaviour of a sandy dike defence in a lake system. In: *Coastal Dynamics: Port of Spain, Trinidad and Tobago*.
- Stive, M.J., de Schipper, M.A., Luijendijk, A.P., Aarninkhof, S.G., Gelder-Maas, C.V., Vries, J.S.V.T.D., Vries, S.D., Henriquez, M., Marx, S., Ranasinghe, R., 2013. A new alternative to saving our beaches from sea-level rise: The sand engine. *J. Coast. Res.* 29, 1001–1008. <http://dx.doi.org/10.2112/JCOASTRES-D-13-00070.1>.
- Stockdon, H.F., Holman, R.A., Howd, P.A., Sallenger Jr., A.H., 2006. Empirical parameterization of setup, swash, and runup. *Coast. Eng.* 53 (7), 573–588.
- Sutton-Grier, A.E., Wowk, K., Bamford, H., 2015. Future of our coasts: The potential for natural and hybrid infrastructure to enhance the resilience of our coastal communities, economies and ecosystems. *Environ. Sci. Policy* 51, 137–148. <http://dx.doi.org/10.1016/j.envsci.2015.04.006>.
- Tonnon, P.K., Huisman, B., Stam, G., van Rijn, L., 2018. Numerical modelling of erosion rates, life span and maintenance volumes of mega nourishments. *Coast. Eng.* 131, 51–69.
- van Bemmelen, C.W.T., de Schipper, M.A., Darnall, J., Aarninkhof, S.G.J., 2020. Beach scarp dynamics at nourished beaches. *Coast. Eng.* 160, 103725.
- van der Meulen, F., Ijff, S., van Zetten, R., 2023. Nature-based solutions for coastal adaptation management, concepts and scope, an overview. *Nordic J. Botany* 2023 (1), e03290.
- van der Meulen, F., van der Valk, B., Baars, L., Schoor, E., van Woerden, H., 2014. Development of new dunes in the Dutch Delta: nature compensation and 'building with nature'. *Source: J. Coast. Conserv.* 18, 505–513. <http://dx.doi.org/10.1007/s>, URL <https://www.jstor.org/stable/24760700>.
- van der Wal, D., 2004. Beach-dune interactions in nourishment areas along the Dutch coast. *J. Coast. Res.* 20 (1), 317–325.
- van IJzendoorn, C.O., Hallin, C., Cohn, N., Reniers, A.J., De Vries, S., 2023a. Novel sediment sampling method provides new insights into vertical grain size variability due to marine and aeolian beach processes. *Earth Surf. Process. Landforms* 48 (4), 782–800.
- van IJzendoorn, C.O., Hallin, C., Reniers, A.J.H.M., de Vries, S., 2023b. Modeling multi-Fraction Coastal aeolian sediment transport with horizontal and vertical grain-size variability. *J. Geophys. Res.: Earth Surf.* 128 (7), <http://dx.doi.org/10.1029/2023JF007155>, e2023JF007155.
- van Koningsveld, M., Mulder, J.P.M., 2004. Sustainable coastal policy developments in the Netherlands. A systematic approach revealed. *J. Coast. Res.* 20 (2), 375–385.
- van Kuik, N., de Vries, J., Schwarz, C., Ruessink, G., 2022. Surface-area development of foredune trough blowouts and associated parabolic dunes quantified from time series of satellite imagery. *Aeolian Res.* 57, 100812.
- van Puijenbroek, M.E., Limpens, J., de Groot, A.V., Riksen, M.J., Gleichman, M., Slim, P.A., van Dobben, H.F., Berendse, F., 2017. Embryo dune development drivers: beach morphology, growing season precipitation, and storms. *Earth Surf. Process. Landforms* 42 (11), 1733–1744.
- van Rijn, L., 1995. Sand budget and coastline changes of the central coast of Holland between Den Helder and Hoek van Holland, period 1964–2040. H2129.
- van Rijn, L.C., 1997. Sediment transport and budget of the central coastal zone of holland. *Coast. Eng.* 32 (1), 61–90.
- van Rijn, L.C., Tonnon, P.K., Walstra, D.J.R., 2011. Numerical modelling of erosion and accretion of plane sloping beaches at different scales. *Coast. Eng.* 58 (7), 637–655.
- van Westen, B., Leijnse, T., de Schipper, M., Cohn, N., Luijendijk, A., 2023. Integrated modelling of coastal landforms. In: *Coastal Sediments 2023: The Proceedings of the Coastal Sediments 2023*. World Scientific, pp. 760–771.
- Warren, I., Bach, H., 1992. MIKE 21: a modelling system for estuaries, coastal waters and seas. *Environ. Softw.* 7 (4), 229–240.
- Zhang, J., Larson, M., 2022. A numerical model to simulate beach and dune evolution. *J. Coast. Res.* 38 (4), 776–784.